AD-A114 451 NAVAL POSTGRADUATE SCHOOL MONTEREY CA F/G 11/6
CHARACTERIZATION OF AN HY-130 STEEL WELDMENT BY TRANSMISSION EL--ETC(U)
DEC 81 W M ELGER

UNCLASSIFIED NL

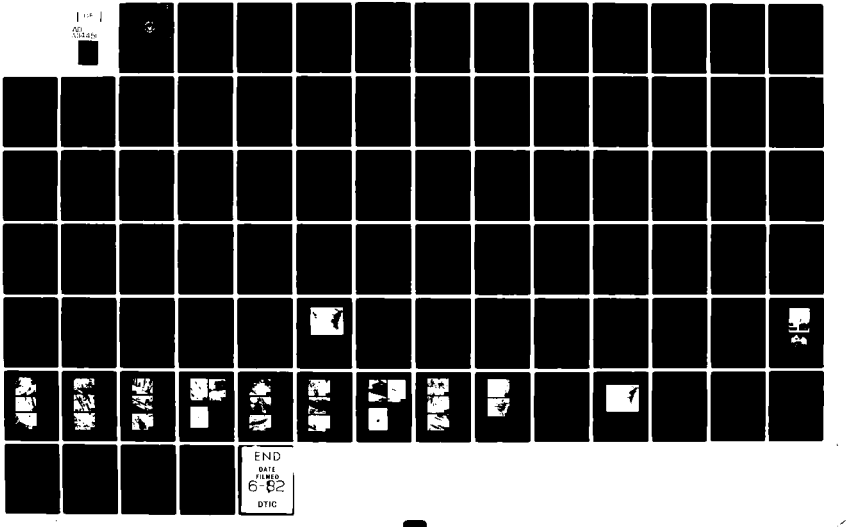

END
DATE FILMED
6-82
DTIC

NAVAL POSTGRADUATE SCHOOL
Monterey, California

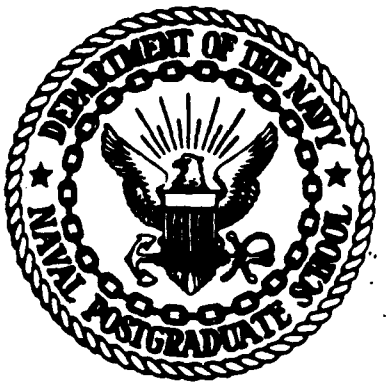

THESIS

CHARACTERIZATION OF AN HY-130 STEEL WELDMENT BY TRANSMISSION ELECTRON MICROSCOPY

by

Wallace Michael Elger

December 1981

Thesis Advisor: K.D. Challenger

Approved for public release; distribution unlimited.

UNCLASSIFIED

SECURITY CLASSIFICATION OF THIS PAGE (When Data Entered)

REPORT DOCUMENTATION PAGE		READ INSTRUCTIONS BEFORE COMPLETING FORM
1. REPORT NUMBER	2. GOVT ACCESSION NO. AD-A114451	3. RECIPIENT'S CATALOG NUMBER
4. TITLE (and Subtitle) Characterization of an HY-130 Steel Weldment by Transmission Electron Microscopy		5. TYPE OF REPORT & PERIOD COVERED Master's Thesis; December 1981
		6. PERFORMING ORG. REPORT NUMBER
7. AUTHOR(s) Wallace Michael Elger		8. CONTRACT OR GRANT NUMBER(s)
9. PERFORMING ORGANIZATION NAME AND ADDRESS Naval Postgraduate School Monterey, California 93940		10. PROGRAM ELEMENT, PROJECT, TASK AREA & WORK UNIT NUMBERS
11. CONTROLLING OFFICE NAME AND ADDRESS Naval Postgraduate School Monterey, California 93940		12. REPORT DATE December 1981
		13. NUMBER OF PAGES 85
14. MONITORING AGENCY NAME & ADDRESS(if different from Controlling Office)		15. SECURITY CLASS. (of this report) Unclassified
		15a. DECLASSIFICATION/DOWNGRADING SCHEDULE

16. DISTRIBUTION STATEMENT (of this Report)

Approved for public release; distribution unlimited.

17. DISTRIBUTION STATEMENT (of the abstract entered in Block 20, if different from Report)

18. SUPPLEMENTARY NOTES

19. KEY WORDS (Continue on reverse side if necessary and identify by block number)

HY-130 Steel Weldment
Transmission Electron Microscopy
Heat-affected zone microstructures

20. ABSTRACT (Continue on reverse side if necessary and identify by block number)

A wrought HY-130 steel weldment was studied to provide information about metallurgical differences in the weld heat affected zone (HAZ). Three GMAW welded areas were mapped and analyzed: heavily tempered, moderately tempered and untempered regions. Transverse sections were cut along the weld HAZ and the section microhardness traverse across the region to determine the location within the HAZ. Transmission electron microscopy revealed the occurrence of significant metallurgical changes from the fusion

DD FORM 1 JAN 73 1473 EDITION OF 1 NOV 65 IS OBSOLETE
S/N 0102-014-6601

UNCLASSIFIED
SECURITY CLASSIFICATION OF THIS PAGE (When Data Entered)

line to the HAZ/base metal interface. Microstructures were found to be similar to those of a low carbon steel, changing from a fine lath martensite at the HAZ/base metal interface to a mixture of upper baimite and fine lath martinsite in the HAZ near the fusion line and finally to lower (acicular) baimite in the weld metal.

Approved for public release, distribution unlimited.

Characterization of an HY-130 Steel Weldment by Transmission Electron Microscopy

by

Wallace M. Elger
Lieutenant, United States Navy
B.S.M.E., United States Naval Academy, 1974

Submitted in partial fulfillment of the
requirements for the degree of

MASTER OF SCIENCE IN MECHANICAL ENGINEERING

from the

NAVAL POSTGRADUATE SCHOOL
December 1981

Author Wallace M. Elger

Approved by: Kenneth A. Shollenberger
Thesis Advisor

Jeff Perkins
Second Reader

Paul C. Martin
Chairman, Department of Mechanical Engineering

William M. Tolles
Dean of Science and Engineering

ABSTRACT

A wrought HY-130 steel weldment was studied to provide information about metallurgical differences in the weld heat affected zone (HAZ). Three GMAW welded areas were mapped and analyzed: heavily tempered, moderately tempered and untempered regions. Transverse sections were cut along the weld HAZ and the section microhardness compared with a previous microhardness traverse across the region to determine the location within the HAZ. Transmission electron microscopy revealed the occurrence of significant metallurgical changes from the fusion line to the HAZ/base metal interface. Microstructures were found to be similar to those of a low carbon steel, changing from a fine lath martensite at the HAZ/base metal interface to a mixture of upper bainite and fine lath martensite in the HAZ near the fusion line and finally to lower (acicular) bainite in the weld metal.

TABLE OF CONTENTS

LIST OF TABLES

LIST OF FIGURES

ACKNOWLEDGMENTS

I wish to express my sincere appreciation to my Thesis Advisor, Dr. Ken Challenger, for his patience and assistance with this work. A debt of thanks is also given to my parents for their encouragement and confidence. Lastly, I wish to especially thank my wife Rosemary for her constant support, understanding and love that sustained me in this effort and throughout my life. I dedicate this work to Rosemary and to my children Meghan and Michael.

Continued financial support by the U.S. Naval Sea Systems Command (NAVSEA) and the helpful comments by Dr. Charlie Zanis at NSRDC are greatly appreciated.

I. INTRODUCTION

A. DEVELOPMENT OF HY-130 STEEL

Since 1960, a continuous effort has been made to develop a submarine hull steel which would give U.S. submarines the ability to operate at significantly greater depths than is attainable with HY-80 steel hulls. Navy requirements called for a steel weldment (base metal, heat affected zone and weld metal) which would exhibit a minimum yield strength of 130,000 to 150,000 PSI, with a high level of fracture toughness at ice water temperatures, good fabricability and good weldability in plate thicknesses up to four inches. [Ref. 1]

A development contract was awarded to U.S. Steel in June 1963 to provide a weldment system which could be produced in existing commercial facilities, and welded with practices that could be utilized in a shipyard. The weldment system encompassed rolled plate, castings, forgings, structural shapes and welding electrodes. The original contract requirements called for the following: [Ref. 2]

1. Uniformity of properties in sections through four inches thick.
2. Adequate ductility to undergo severe cold forming.
3. High resistance to shear tearing.

4. Ductile behavior under impact loading at 30°F.

5. Minimum susceptibility to the Bauschinger effect.

6. Adequate resistance to low-cycle, high strain fatigue.

7. Minimum susceptibility to stress-corrosion cracking, corrosion fatigue, and general corrosion in sea water.

8. Satisfactory weldability under shipyard conditions.

9. Feasibility for production on current commercial facilities.

10. Economic feasibility.

The Applied Research Laboratory at U.S. Steel developed a 7½ Ni-Cr-Mo Steel with 150,000 PSI yield strength which met most of the requirements set forth in the Navy contract awarded in June 1963; however, prospects for a suitable weldment system were believed to be much better in the 130,000 PSI yield strength range. To this end, a 5¼ Ni-Cr-Mo-V steel developed by International Nickel Company in this 130,000 PSI yield strength range was selected as a baseline material. [Ref. 1]

From June 1963 until July 1966, U.S. Steel conducted an extensive development and testing program to establish compositional limits, through refinement of the alloy including residual element effects, melting effects, rolling-ratio effects and forming effects on this 5¼ Ni-Cr-Mo-V steel alloy called HY-130. The optimum chemical composition was found to be as follows: [Ref. 2]

Element	Weight Percent
Ni	4.75 - 5.25
Cr	.40 - .70
Mo	.30 - .65
V	.05 - .10
C	.10 - .12
Mn	.60 - .90
Si	.15 - .35
Cu	.25 Max.
Ti	.02 Max.
P	.01 Max.
S	.01 Max.
Fe	Balance

B. INFLUENCE OF ALLOYING ELEMENTS ON HY-130 PROPERTIES

The resulting influence of the major elements on the HY-130 steel was studied by varying the amount of a single element, and analyzing the resulting change on the alloy properties, due to that element.

Nickel is primarily used as a hardenability addition. It contributes to the solid solution strengthening of the steel, but it is also found to be particularly effective in lowering the nil-ductility transition temperature (NDT) and may be added in large amounts without embrittling quenched and tempered HY-130 steel. The five percent nickel content was found to produce an NDT temperature of

-120°F. Larger amounts of nickel would lower the NDT temperature even further, but would also lower the shear energy absorption. [Ref. 3] Lastly, five percent nickel was deemed to be the optimum content required to balance hardenability and weldability.

Chromium is a strong carbide former in HY-130 steel, and is added to increase hardenability and to produce secondary hardening of the steel during heat treatment. Chromium content is kept at .40-.70 weight percent to prevent the possible embrittling effects encountered with higher percentages. [Ref. 2]

Molybdenum is also a strong carbide former and is added for both hardenability and as a secondary hardening agent. Molybdenum contributes to secondary hardening in such a way that the strength of the steel can be conveniently varied by adjusting the weight percent from .30-.65. It should be noted that when the sum of manganese and molybdenum exceed 1.5 weight percent or the sum of manganese, molybdenum and chromium exceeds 2.5 weight percent, the notch toughness of the steel is adversely affected. [Ref. 2]

Vanadium is primarily added to the HY-130 steel alloy to prevent softening during tempering at temperatures up to 1100°F. The optimum weight percentage of Vanadium was found to be .07 weight percent, for which the yield strength of the alloy remains essentially constant in the

range of $900^{o}F$ - $1100^{o}F$. [Ref. 2]

Carbon content is maintained in the range of .09-.12 weight percent. For adequate yield strength, high notch toughness, and good weldability, carbon is the major contributor to cracking and must be kept as low as possible, consistent with the 130,000 PSI yield strength requirements. [Ref. 3]

Silicon is used to control the oxidation taking place during the melting and refining process used to make the HY-130 steel, and it has been found that silicon levels must be kept low in order to avoid a decrease in notch toughness. [Ref. 4] The specification for HY-130 steel calls for between .15-.35 weight percent due only to the difficulty in maintaining control of the state of oxidation of the steel during the final stages of the melting when silicon content is low, and still produce HY-130 steel using conventional techniques. [Ref. 2]

Manganese significantly increases the hardenability of HY-130 in the range of .60-.90 weight percent, but is limited to .90 weight percent due to decreasing notch toughness of the steel. [Ref. 2]

Phosphorous is an impurity element present in the making of steel and it must be kept below .01 weight percent to prevent temper embrittlement, especially if the HY-130 plates are not quenched after tempering. [Ref. 2]

Sulfur is extremely detrimental to notch toughness and preferably must be kept below .008 weight percent. Usually, the combined effect of sulfur and oxygen is of concern with respect to notch toughness, and O_2 limits of 35PPM are established. [Ref. 2]

Aluminum is added to ensure that the HY-130 steel is fully killed, and the range of .015-.035 weight percent will ensure low oxygen content, and a significant improvement in toughness without the formation of Aluminum-Nitrite precipitates. [Ref. 4]

C. INFLUENCE OF HEAT TREATMENT ON HY-130 PROPERTIES

HY-130 steel requires a tempered martensitic microstructure to achieve the required combination of strength and notch toughness. The design of HY-130 steel is such that hardenability is sufficient to ensure the desired mechanical properties set forth in the Navy development contract. From the Isothermal-Transformation diagram for HY-130 steel (Fig. 1) it is seen that the transformation to ferrite is suppressed to times in excess of 10^4 seconds, however, the transformation to lower bainite occurs in as short a time as 20 seconds below the Ms temperature. As a result, thick plates of HY-130 exhibit mixed microstructures of bainite and tempered martensite. Double austenitizing heat treatments are recommended for 2-inch and larger plates, to help improve uniformity of mechanical properties and notch toughness.

HY-130 steel has a high tempering resistance. It has been shown that higher tempering temperatures result in a decrease in strength, therefore the tempering temperature for 2-inch thick plate is limited to 1150^{o}F to maintain the minimum 130,000 PSI yield strength.

D. WELDABILITY OF HY-130

HY-130 steel has been shown to have adequate hardenability to form a martensitic heat affected zone (HAZ) structure upon welding, with heat input energy levels of 50 KJ/in. When welded using the gas metal arc process (GMA) in a spray transfer mode, hydrogen content of the welding wire should be below 3ppm to prevent embrittlement. [Ref. 5]

Filler materials for use with HY-130 steels have been developed to match base plate properties. Because of the solidification cycle through which the weld fusion zone must pass and the lack of any postweld heat treatment, the weld metal composition has been selected to produce an as-deposited yield strength of about 140,000 psi.

E. EXPLOSION BULGE TEST QUALIFICATION

The procurement specification for HY-130 steel plate and castings is a rigorous system of procedures to help ensure that the material meets the required toughness, mechanical properties, strength and weldability for naval applications. The explosion bulge test (EBT) is required

for the preproduction series of cast HY-130 pieces to check the toughness of the as-welded material. The explosion bulge test is a Navy requirement used to evaluate the acceptability of the base metal, weld metal, and heat affected zone of the weldment system, prior to its final acceptance and installation on naval vessels.

Test plates for an HY-130 explosion bulge test are formed from two 30" X 15" plates that are joined along their length by a gas metal arc welding, spray transfer process using a filler material of 140,000 psi yield strength. The welded 30" X 30" plates are then placed on a circular ring with an inside diameter of 18". The temperature of the plate is set so that the sample is on the upper shelf of the ductile to brittle transition temperature (DBTT). An explosive charge is placed 15" above the mid point of the plate and then detonated. After the explosion, the reduction in plate thickness at the bulge apex, and any damage is noted. Failure determination of the weldment is a complex process and is covered in [Ref. 6]

The Explosion Bulge Test procedure for HY-130 steel has been reported on by Rathbone. [Ref. 7] He found that there was a frequent occurrence of fractures along the edge of the fusion zone, through the heat affected zone. Similarly, Brucker, [Ref. 8] reported that the fracture in the EBT HY-130 plate initiated in the HAZ.

F. PREVIOUS RESEARCH

The observation by Brucker [Ref. 8] that a hardness traverse across an HY-130 weldment exhibited a very rapid change in the transition region between the HAZ and base metal. This region was termed a "metallurgical notch," and appeared to assist crack initiation and subsequent failure during the EBT of some plates. Brucker hypothesized that the low hardness, low strength region of the HAZ would attempt to deform during EBT, but would be restrained from doing so by the much stronger material adjacent to it (higher hardness), thus creating a triaxial stress state in the region.

Sorek [Ref. 9] examined the thermal history of an HY-130 weldment and studied the magnitude of tempering which was produced by initial and subsequent GMAW weld passes. Light microscopy was utilized to correlate metallurgical features with predictions made using information obtained from thermocouples and strip chart recordings of thermal cycling upon welding.

G. SCOPE AND OBJECTIVES OF PRESENT WORK

The present research effort results from a recommendation outlined in Sorek's paper to:

> "Perform an in-depth, qualitative study of the tempering effects of both straight and temper bead sequences on the weld heat affected zone through the use of transmission electron microscopy."

Thin foil transmission electron microscopy has been

utilized to study the heat affected zone microstructure of an HY-130 steel weldment in order to gain an understanding of the resultant microstructural changes which occur upon welding.

II. BACKGROUND

Studies on HY-130 weldments utilizing transmission electron microscopy are not readily found in published literature. Much work has been published since 1963 on HY-130 utilizing light microscopy for studying base plate microstructures, and to a much smaller degree, using scanning electron microscopy to conduct fractographic studies on HY-130 weldments.

A. REVIEW OF PREVIOUS STUDIES OF HY-130 UTILIZING TRANSMISSION ELECTRON MICROSCOPY

The development of HY-130 steel as it is known today, took place at the U.S. Steel Research Laboratory in Monroeville, Pennsylvania, and the first TEM study on HY-130 was conducted by Porter and Paulina [Ref. 10] in 1968. Thin foils were made of rolled base plate material taken at the plate surface and midthickness. Studies were done on both as-quenched, and quenched and tempered specimens.

The quenched and tempered HY-130 rolled plate showed similar microstructures at both the surface and mid-thickness of a 5.2cm thick plate; a lath-like ferritic matrix with fine carbides throughout, indicative of a tempered martensitic microstructure. Relatively coarse carbides were also found on some of the prior austenite

grain boundaries, with a smooth appearance of the ferrite in those regions, indicative of a bainitic structure.

Porter and Paulina commented on the difficulty of distinguishing between bainite and tempered martensite in HY-130. This is due to the high martensite start (M_s) temperature, which allows for self-tempering of martensite to occur in martensitic regions during cooling from the M_s temperature. Martensite was found to be darker in appearance as a result of carbide precipitation. Bainite was distinguished as areas of black resolvable carbides with white patches of ferrite. The distinction between martensite and bainite was postulated by studying as-quenched HY-130 microstructures.

As previously stated, examination of HY-130 weldments by transmission electron microscopy has not received much attention in the literature; however, the following two studies on HY-130 weldments using transmission electron microscopy provide some limited background information.

Boniszewski and Watkinson [Ref. 11] conducted a study of HY-130 microstructures to determine whether a particular microstructure was susceptible to hydrogen embrittlement. The heat affected zone of a HY-130 weldment was found to exhibit microstructures of lath bainite, lath martensite and pockets of twinned martensite. Twinned martensite, which is normally not found in such a low (0.1%) carbon steel, was found to exist in small pockets, which would be

feasible if: a higher local cooling rate existed; or the carbon content, due to segregation, was greater than 0.25% in small regions.

Chen and Thompson [Ref. 12], conducted a study on HY-130 weldments, concentrating on the area near the fusion line for examination with the transmission electron microscope. The predominant microstructures observed were martensite and bainite, with a variety of forms and sizes. Retained austenite was found in several areas, although it was present in relatively small amounts when compared to the predominantly martensitic and bainitic strucutres. This retained austenite was found only in the GMAW welds, but the factors underlying this result were not explained. Carbides were found in a number of the microstructures and the morphology of the carbides was found to be similar to those seen in lower bainite (elongated rods). Reflections from the carbides were extremely faint, and therefore conclusive identification was not made.

The martensite start (M_s) temperature for HY-130 GMAW welded steel was reported as 432°C by Chen and Thompson. Since the martensitic transformation occurred at a relatively high temperature, one would expect to see only bainite I and martensite in the microstructure, but bainite III was also observed. This transformation to lower bainite was not accompanied by retained austenite. For the bainite III, it was observed that as the

tranformation temperature decreased, the bainitic lath spacing narrowed, and carbides were precipitated at the lath boundaries as well as in the interior. Bainite I was characterized by wide bainitic laths with retained austenite found either at the lath boundaries, or in small islands within the laths themselves. Carbides were precipitated at dislocations in the bainite I, in sharp contrast to carbides forming at lath boundaries and interior regions in bainite III. The martensitic microstructure was found to contain extremely fine carbides which were visible only at high magnification and under dark field image conditions. The martensite twins observed were found within wide bainitic laths and were thought to have occurred as a result of solidification segregation.

B. REVIEW OF THE EFFECTS OF QUENCH RATE ON LOW CARBON MARTENSITE

The microstructure of steel is strongly influenced by the cooling rate experienced as it proceeds from a high temperature regime, where it is completely austenitic, to a low temperature regime. The HAZ of HY-130 steel undergoes a high-to-low temperature cycling during the welding process, and the intent of this work is to examine the microstructural changes within the HAZ, due to welding thermal cycling. At present, a model to predict the microstuctural changes that HY-130 undergoes during this thermal cycling does not appear in the literature. For

this reason, it is felt that an examination of the changes experienced by a low carbon martensite would provide a starting point to help study the microstructure of HY-130 subjected to complex thermal cycling.

Ansell and Donachie [Ref. 13] examined the changes in low carbon martensite due to various quench rates for Fe-Ni-C steels. The information which was presented can be compared to weld HAZ's, although much slower quenching is experienced by HY-130 (0.1%C) during cooling from welding temperatures. For quench rates just exceeding the critical cooling rate, sufficient time is available between the austenitizing temperature and the M_s temperature for carbon to segregate to imperfections (dislocations and grain boundaries). Since the size of those regions is a maximum at the eutectoid temperature, optimum strengthening of austenite is obtained. Austenite is therefore more resistant to the shear during the transformation to martensite, thus the regions of carbon segregation are inherited by the martensite and serve as suitable sites for carbide formation.

The work of Ansell and Donachie also characterized the morphology of the martensite observed under relatively slow cooling conditions, similar to those encountered in the cooling of a weldment. Massive martensite was found to be the predominant morphology of the slow cooled microstructure, which can be characterized by packets of fine

parallel laths containing a high density of dislocations with very little retained austenite. The width of the parallel laths became thinner with higher quench rates. Increasing the quench rate was also found to decrease the size of the Widmanstatten carbides present in the Fe-Ni-C alloy and to decrease the thickness of any martensite twins which were formed, however, the number of twins which were formed was found to increase.

C. REVIEW OF TEMPERING EFFECTS ON LOW CARBON MARTENSITE

Speich [Ref. 14] reported that 90 percent of the carbon segregates to dislocations and lath boundaries during quenching in the study of .026%C and 0.18%C martensites. Since the carbon content is saturated in the martensite, it acts as a nucleus for carbide growth. It was further reported that alloying with nickel had a 25-fold greater enhancement of carbon diffusivity than for pure gamma iron, thus requiring a much faster quench to limit carbon segregation in HY-130.

Speich's work corroborates with the results shown by Ansell and Donachie [Ref. 13] that the carbon segregation acts as a nucleus for carbide growth. It was further reported by Speich that during tempering at less than 150°C carbon segregation is occurring in the martensite, but no carbides are formed. As the tempering temperature is raised into the 200°C to 330°C range, a rod-shaped carbide is precipitated. At tempering temperatures above 400°C, a

spheroidal Fe_3 C carbide is precipitated both within and between the martensite laths. Once again, Speich could not conclusively identify the rod-shaped carbide precipitated at 250°C by selected area diffraction, but he was able to verify that the spheroidal carbide precipitated at 400°C was Fe_3C.

III. EXPERIMENTAL PROCEDURE

A. MATERIAL

Three heats of HY-130 steel were used in the study. One heat was provided by the Naval Sea Systems Command (NAVSEA) from their inventory at the Mare Island Naval Shipyard (MINSY) which was a rolled 50mm thick plate, heat # 5P4184, with composition and heat treatment data presented in Tables (1 & 2). The other two heats were cast as a 50mm thick plate, heats #21327, #36615 and further referred to as plates #4 and #6 in the paper by Brucker. [Ref. 8] Two pieces of each heat 38.1cm. X 76.2cm. were GMA welded into a 76.2cm square using 140,000 PSi yield strength filler wire by MINSY. The GMA welds were made using a heat input of 52,000 joules per inch as recommended by Connor and Rathbone [Ref. 3] and preheat temperature was maintained at 120°C. The rolled plate was used by both Brucker [Ref. 8] and Sorek [Ref. 9] for their studies of an instrumented HY-130 weldment. The cast pieces (plate #4 and #6) were explosion bulge tested prior to this study. The qualification mechanical properties are given in table (3).

B. INITIAL PREPARATION OF PLATES

Sections of the rolled plate were cut by Sorek [Ref. 9] for his use in the microhardness evaluations of the weld metal, HAZ and base metal. The sample used in this study

was a subsequent 10mm section cut from the same rolled plate. This section was then polished using standard metallographic procedures to produce a surface which was optically flat at 600x. The section was then etched using an Ammonium Persulfate solution ($10g(NH_4)_2(SO_4)_2$ in 90ml. H_2O) using a swab-water rinse-swab technique to reveal the various weld passes, fusion line and visible HAZ. The HAZ appeared in dark contrast to the fusion line and the weld metal. Both sides of the specimen were prepared in this manner. Measurements were then taken to show a good correlation between the location and size of the HAZ on both sides, thus indicating that the fusion line and HAZ were essentially straight in this 10mm section. Plates #4 and #6 were prepared in the same manner. Photographs were taken of the rolled plate and the contrast between weld metal, visible HAZ and base metal are shown in Figure (2).

C. MICROHARDNESS MEASUREMENTS

Several microhardness traverses were conducted by Sorek [Ref. 9] on the rolled plate, and several microharness traverses were conducted in this work on the cast plates (plate #4 & #6) and individual readings on slices taken from the rolled plate. The microhardness traverses across the weldment were conducted to establish a microhardness "map" across the HAZ for use in pinpointing the the location that each thin foil represents within the HAZ region. These microhardness traverses are shown in Figures (3-9).

Microhardness measurements were made with a Buehler microhardness tester, using a diamond indenter, 200g load, and 600x optical system. Readings were taken with sufficient spacing so as to accurately capture the slope of any hardness gradients. All distances shown on the figures (3-9) are in millimeters distance from the fusion line. Three separate regions were selected for examination on the rolled plate, and one region on each of the cast plates. For the rolled plate (figure 2), region #2 is the HAZ along the right hand side of the weldment center, corresponding to the hardness traverse shown in figure (3). Region #3 corresponds to the last weld pass HAZ, on the lower left of the weldment in figure (2), corresponding to the hardness traverse shown in figure (5). Region #4 corresponds to the fourth from last weld pass HAZ, lower right in weldment figure (2), with associated hardness traverse shown in figure (4).

D. SECTIONING MATERIAL ALONG THE HAZ

The cutting of slices of metal across the HAZ at carefully selected distances from the fusion line was the first step in the production of thin foils, which would later be examined in the transmission electron microscope. Each region described in figure (2) was cut from the 10mm thick transverse weldment section to a size which could be mounted in a South Bay Technology low speed wafering saw. (Figure 10). These smaller sized pieces which contained

portions of the weld metal, HAZ and base metal were then carefully sectioned into 0.3mm. nominal thickness slices using a low speed diamond wafering blade. Each slice was marked and placed in a dessicator for later use.

E. METHOD OF DETERMINING THIN FOIL LOCATION IN HAZ

A two step process was utilized in determining the thin foil location in the HAZ. First, a detailed accounting system was kept for each region with the aid of the low speed wafering saw micrometric feed assembly, and the knowledge that kerf loss between cuts was 0.3mm. Second, microhardness readings were made on both sides of the slices and recorded. By using the mechanical measurement from the micrometric feed assembly and the hardness measurement for an individual slice, a comparison could be made with the microhardness traverse "map" previously discussed. This comparison provided a positive means of locating a slice within the HAZ, and consequently the thin foils manufactured from that slice would show the representative microstructure at a known distance away from the fusion line. Accuracy of the measurments was $\pm$ 0.1mm. Plots of each slice along the microhardness "map" for their respective region are shown in figures (3-6).

F. THIN FOIL PREPARATION

Preparation of extremely thin foils of HY-130 for observation in the transmission electron microscope (TEM)

were essential to this work. Since HY-130 steel is a magnetic material, the volume of material must be kept to a minimum to avoid interference (astigmatism) of the electron beam due to the magnetic fields generated from the specimen. A Struers Tenupol electropolisher and a FTS Multi-Cool methanol refrigerating unit (figure 10) were utilized in foil preparation. After the individual sections were cut, and microhardness measurements were taken, the slices were electrothinned to .05mm. nominal thickness using the Tenupol polisher, 10mm. diameter specimen holder and an electrolyte consisting of 5% perchloric acid and 95% acetic acid. This electrothinning solution was kept at a working temperature of 15°C by recirculating a refrigerated methanol solution through cooling coils in the Tenupol unit. Throughout the preparation of the thin foils, polishing was found to significantly deteriorate as the temperature of the electrothinning solution climbed above 20°C. At temperatures just below 15°C acetic acid freezes and thus the temperature of the solution must be maintained between 15 and 20°C.

Disks of 3mm. diameter, .05mm. thickness were then electrolytically cut from the larger slice. Special acid resistant tape was used to cover one side, and disks of 3mm. diameter, from the same type of tape, were affixed to the other side of the thinned slice, and subsequently material from around that disk was electropolished away. The 3mm.

disks then required very careful handling so that the foil would not be bent in any way. The acid resistant tape and adhesive disks were removed by soaking the foil in acetone until the adhesive dissolved and the tape floated free. Although the method of electrocutting the disks from each slice was a tedious process, it was found to be superior to mechanically punching out disks, which caused considerable distortion.

Final electropolishing of the disks was carried out using a 3mm. diameter specimen holder and a photocell--rheostat-controlled light source to terminate polishing upon penetration. Current density in the percholoric-acetic acid solution for electrothinning and electropolishing was set at 5ma per square millimeter. Flow rate was set on high speed for electrothinning and electrolytic cutting and on low speed for final electropolishing. Foils were stored in glass bottles inside a dessicator until needed. Further details of the electrothinning, electrolytic cutting and electropolishing are contained in Appendix A.

G. OBSERVATION IN THE TRANSMISSION ELECTRON MICROSCOPE (TEM)

Observation of HY-130 thin foils was conducted on a Philips EM201 electron microscope at 100kv acceleration voltage. This electron microscope was designed and equipped for the study of marine biological specimens and

did not possess a tilting goniometer stage. This electron microscope also did not have satisfactory objective apertures for dark field microscopy nor were the field limiting apertures for selected area diffraction satisfactory. These deficiencies limited the amount of quantitative diffraction analysis that could be performed on the HY-130 samples.

H. ATTEMPTS AT TRANSMISSION ELECTRON MICROSCOPE STUDIES OF HY-130 CAST MATERIAL

It should also be noted at this point that thin foils of the HY-130 cast material (plate #4 and #6) could not be manufactured successfully using the same technique successfully demonstrated for the rolled material due to the inherent porosity in the cast material. Regions near the pores and in the pores themselves tended to polish preferentially, and revealed only thick-edged, irregular holes when observed in the TEM.

IV. RESULTS AND DISCUSSION

A. SPECIMEN LOCATION WITHIN MICROHARDNESS TRAVERSE

The relative distance of each thin foil taken within the HAZ was measured in millimeters from the fusion line. The method of locating each thin foil utilized both mechanical measurement microhardness readings with the results plotted in figures (3-6). These figures show the microhardness "map" of the HAZ and each dot represents a location where a slice was taken for later processing and observation in the TEM. The excellent correlation between mechanical measurement and microhardness readings on each section, and the corresponding microhardness "map" indicate that the location of a thin foil within the HAZ is known to within $\pm$ 0.1mm.

B. COMPARISON OF MICROHARDNESS TRAVERSES

The idea of a metallurgical "notch," postulated by Brucker [Ref. 8] suggests that a large change in hardness over a short distance, as is sometimes seen in the HAZ of weldments, presents essentially a notch favoring the formation of a crack in a weldment upon loading. For the rolled plate, region #2, as shown in figure (2) and figure (3), the decrease in hardness from a high of 400 vickers hardness (HV) to a low of 315(HV) over a distance of 3.0mm. indicates that a metallurgical notch in this region would be very slight, and will not present difficulties with

weldment toughness. This gently sloping hardness gradient results from the tempering that region #2 receives from several nearby welding passes.

The rolled plate, region #4, as shown in figure (2) and figure (4), shows a change in hardness from 385(HV) to 290(HV) in a distance of 0.75mm. and this relatively steep hardness gradient might pose some difficulties with weldment toughness. The region received only one tempering pass after the initial weld pass. It should be pointed out that region #4 is located on the straight bead sequence weldment side and is in the location of the first pass of the final four weld passes.

Rolled plate region #3, shown in figure (2) and in figure (5), shows the steepest hardness gradient of the three rolled regions examined. From a hardness value of 390(HV), the decrease in hardness to 277(HV) occurs in 0.5mm. distance. This very steep hardness gradient would pose severe difficulties with weldment toughness. It can be seen from figure (2) that region #3 received no tempering from other weld beads, resulting in the steep hardness gradient. Region #3 was the last pass in the straight bead sequence weldment side.

Cast plates #4 and #6 posed difficulties in the production of thin foils for examination with the TEM, as previously discussed, but were examined with the microhardness tester and results are presented in figures (6-9).

Plate #6 was welded with the temper bead sequence, and the hardness is shown to decrease from 415(HV) to 310(HV) in a distance of 2.0mm. This is a gently sloping hardness gradient, and would not be a serious metallurgical notch, thus having little effect on weldment toughness. The second microhardness traverse of plate #6 showed essentially the same gently sloping hardness gradient as before, but the distance from maximum to minimum hardness was 1.75mm.

Cast plate #4 was welded using a straight bead sequence only, thus comparison with cast plate #6, welded with the temper bead sequence only, might indicate whether one welding sequence could produce a more severe metallurgical notch. The measured hardness in the region of the final weld pass of plate #4 is shown in figures (8-9). The hardness changes from 396(HV) to 325(HV) in 0.25mm. and from 391(HV) to 312(HV) in 0.25mm. distance, indicating an exceptionally steep hardness gradient. This severe hardness gradient would pose difficulties with weld toughness and is an excellent example of a metallurgical "notch."

C. EXAMINATION OF INDIVIDUAL SECTIONS WITHIN THE HAZ

The three rolled plate regions (#2, #3, #4) were examined with the transmission electron microscope to gain an understanding of, and to characterize, the microstructures found within a HY-130 GMAW weldment heat affected zone. Sections examined were: the base metal; 3.25mm., 2.5mm., 1.5mm., and 1.0mm. from the fusion line;

the fusion line itself; and the weld metal just inside the fusion line. Figures (11-19) provide an easy comparison of the above listed sections, as an individual section from one region is presented with its corresponding section from the other two regions.

1. Base Metal

The base metal was examined in the transmission electron microscope to provide a known baseline microstructure. The microstructures presented in figure (11) show several prior austenite grain boundaries, and large spheroidal carbides are seen at those prior austenite grain boundaries and at lath boundaries. The microstructure is indicative of a tempered martensite with large spheroidal carbides. The martensite laths contain a moderately high dislocation density. Lath spacings have been calculated for these specimens and the other specimens and are presented in table (5).

2. 3.25mm. from Fusion Line

The next set of sections examined are those representing the HAZ at a distance of 3.25mm. away from the fusion line. There are fewer large carbides visible in these sections, (figure (12)) than in the initial tempered martensite. Finer lath new martensite is present. Region 4 contained a very small amount of granular bainite, however this was not a general characteristic of any of these sections. Regions 2 and 3 show a predominantly fine

heavily dislocated martensitic microstructure, but the large carbides are still visible, the hardness of all the regions show that they represent the HAZ region nearest the base metal.

3. 2.5mm. from Fusion Line

Changes begin to appear in the next region which represents the HAZ at a distance of 2.5mm. away from the fusion line, figure (13). Although the predominant microstructure is still martensite, very few large carbides are visible, and region 3 shows bainite I (upper bainite) with Widmanstatten carbidea in a wide bainitic lath as sharply contrasted to the narrow lath spacing of the martensitic microstructure. Region 4 shows some granular bainitic microstructure within a predominantly martensite and bainite I field. Region 2 shows martensite with an occasional ferrite region bordering the martensite-bainite interface. Large carbides encircle the ferrite, and retained austenite is also suspected in this region. Figure (14) shows a ferrite, and typical microstructure of region 3 with the wide bainite I laths shown in contrast to the martensitic microstructure. Within the bainite, large regions of rod-shaped Widmanstatten carbides are present along with marteniste. The photo at the right is an enlarged view of the Widmanstatten carbides within an upper bainite region. The corresponding diffraction pattern is shown in figure (14) with the very faint carbide reflections present near the central spot.

4. 1.5mm. from Fusion Line

The region examined represents the HAZ at a distance of 1.5mm. away from the fusion line (figure (15)). The large spherical carbides are no longer present. The rod-shaped Widmanstatten carbides have replaced the spheroidal carbides in a predominantly bainite I microstructure. Region 2 shows highly dislocated lath martensite with a finer lath spacing than previously observed. Large regions of bainite are the dominant microstructural features in regions 3 and 4 with region 3 showing very few carbides in the bainite in sharp contrast to the high density of rod-shaped Widmanstatten carbides shown in region 4 in the fairly wide bainite lath. Twins are attributed to segregation of alloying elements in the relatively slow cooled weldment, and are not a dominant feature of this section.

5. 1.0mm. from Fusion Line

Bainite I comprises a large fraction of the microstructure in regions representative of the HAZ at a distance of 1.0mm. away from the fusion line. (Figure (16)) The large regions of bainite and the associated rod-shaped Widmanstatten carbides are shown in sharp contrast to the highly dislocated lath martensite. Region 3 shows the relatively wide bainitic laths and the narrow martensitic laths with retained austenite being suspected at the lath boundaries. Region 4 clearly shows the rod-shaped Widmanstatten carbides precipitated at dislocations within

the wide bainite I laths. Figure (17) shows the dark field-bright field microstructures from a region of section 4 with the presence of twinned martensite in the wide laths encompassing the Widmanstatten carbides. This twinning is not characteristic of such a slow cooled weldment, but is known to occur in bainite I as a result of alloy segregation. [Ref. 11] The associated selected area diffraction pattern reveals this twinned martensite and is shown in the same figure.

6. Fusion Line

The fusion line region is shown in figure (18) and for the first time. Bainite III (lower bainite) is observed. The acicular bainite laths show some carbides at boundaries and interior regions. The amount of carbides visible has greatly decreased from those seen in other regions of the HAZ, and the laths are narrower and shorter than those of bainite I.

7. Weld Metal Just Inside Fusion Line

The weld metal just inside the fusion line was examined and figure (19) shows the representative microstructure for this region. The miscrostructure is predominately bainite III with no carbides visible in the photographs. The lath spacing is wider than that observed in the fusion line region, but the bainite laths are not as wide as those observed in bainite I.

D. DISCUSSION OF MICROSTRUCTURE FOR INDIVIDUAL SECTIONS

1. Base Metal

The base metal microstructures, figure (11), exhibited a tempered martensitic appearance, where the heavy tempering of the base metal prior to welding allowed large spheroidal carbides to be formed. The tempering temperature was held at 620°C for three hours, followed by a water quench. Speich (Ref. 14] showed that a tempering temperature of 400°C for three hours was sufficient for the formation of spheroidal carbides of Fe_3C to form in a low carbon martensite (0.1%C) and this effect is seen in the microstructure of the HY-130 base metal region.

2. 3.25mm. from Fusion Line

The region of the HAZ that is 3.25mm. distant from the fusion line is shown in figure (12). This region shows fewer large carbides than were visible in the base metal, indicating that some of the large carbides went into solution as the temperature in this region reached approximately 760°C, as shown in figure (20). The temperature reached in this region was not high enough to dissolve all the large carbides, therefore the austenite which was formed had a lower carbon content than would normally be expected for a 0.1% carbon steel. The martensite start temperature (Ms) is therefore raised, making it more difficult for bainite to form upon cooling.

3. 2.5mm. from Fusion Line

The changes which appear in the regions representing the HAZ at a distance of 2.5mm. away from the fusion line, figure (13), result from the large carbides being almost completely solutioned as the temperature in the region was near 880°C. As the number of large carbides that are solutioned increases, the amount of carbon in solution in the austenite increases, thus lowering the Ms temperature and making it easier for bainite to form. Upon cooling from 880°C, bainite I is formed along with Widmanstatten carbides in the regions where large alloy carbides once appeared. Carbides may be present in the martensite, but if so, are too small to be seen at the magnifications used in this work. (Figure (14)). However, carbides may not be formed, as Speich [Ref. 14] reports that at temperatures below 150°C, carbon segregation in a 0.1%C martensite occurs without the precipitation of any carbides. The preheat and postheat temperature of the weld is 120°C, and since the Ms temperature is reasoned to be lower in this region due to more carbon in solution, no rod shaped carbides were formed in the martensite. Also, since the Ms temperature is lowered in this region, the kinetics for self-tempering of martensite in this region are not favored. Retained austenite in this region is suspected, but due to difficulties with selected area diffraction apertures explained earlier, it could not be proven.

4. 1.5mm. from Fusion Line

The mixture of bainite I - martensite microstructure in the region of the HAZ at 1.5mm. away from the fusion line, (figure (15)), can be reasoned by referring to the iso-thermal transformation diagram for HY-130 steel, figure (1). For a martensite start temperature (Ms) of 482°C, less than five percent bainite will form in three minutes. Since no large carbides are present in the microstructures, a larger amount of carbon must be in solution than in the previous sections which would lower the Ms temperature, thus allowing a larger amount of bainite to form. The bainite was formed upon cooling from the 1020°C peak temperature experienced in this region during welding and large rod-shaped Widmanstatten carbides were also precipitated within the bainite during the transformation from austenite. Lath martensite is still present in this region, as predicted by the transformation diagram, but the lath spacing is smaller due to the higher cooling rate experienced nearer the fusion line.

5. 1.0mm. from Fusion Line

The region of the HAZ that is 1.0mm. away from the fusion line, figure (16), is much like that of the previous region with bainite I and martensite being the predominant microstructure. There are large numbers of rod-shaped Widmanstatten carbides precipitated at dislocations within the bainite laths, and a smaller number of rod-shaped

carbides appear in the narrow martensite laths, indicating some autotempering may have occurred. Twinned martensite was occasionally found in this region, probably due to alloy segregation, figure (17). There is some retained austenite suspected in this region, which is reasonable when the rapid cooling rate from 1170°C experienced by this region is considered. Chen and Thompson [Ref. 12] illustrate similar micrographs of retained austenite in their work, especially in regions of upper bainite.

6. Fusion Line

The sections representing the fusion line, as shown in figure (18), are subjected to a temperature of approximately 1536°C. The microstructure consists of primarily lower bainite. Carbides are not visible and, since the temperature (1536°C) would be high enough to ensure complete solutioning of the carbon and the possibility of some mixing with weld metal, the Ms temperature would be lower at the fusion line than for any other region of the HAZ, thus allowing lower bainite to form. The cooling rate in this region is fairly rapid, and is at least 17°C per second given by Sorek, [Ref. 9] which exceeds the 8°C per second cooling rate required for martensite formation as discussed by Holsberg. [Ref. 15] Another explanation for the lower bainite present at the fusion line is that dilution of the base metal (5% nickel) probably occurred, mixing with the weld metal (2.76%nickel) producing a lower hardenability and

lower Ms than that shown in the isothermal transformation diagram. Composition ranges for base metal and filler metal are given in tables (1) and (4).

7. Weld Metal Just Inside Fusion Line

The miscrostructures representing the weld metal, as shown in figure (19), are similar to the microstructures at the fusion line, thus indicating that the region thought to be weld metal only was actually a similar dilution of weld metal and filler metal. Stoop and Metzbower [Ref. 16] have verified this dilution in the fusion zone by microprobe analysis. Referring to figure (21) showing the weld geometry superimposed on a macro photograph of the etched weldment, it is clear that a region of weld metal only, undiluted with the base metal, lies well inside the fusion line toward the weld center. This would explain the similarity in the microstructures representing the two regions.

V. ADDITIONAL REMARKS

The objective of this work was to characterize the HAZ microstructures in a GMAW weldment of HY-130 steel utilizing transmission electron microscopy. It was felt that this characterization could be used to support work carried out by others in the solution of the two major problems in HY-130 weldments: hydrogen embrittlement or stress corrosion cracking, and low HAZ fracture toughness. The following remarks address these issues.

Throughout the literature covering hydrogen embrittlement or stress corrosion cracking (SCC) in HY-130 weldments, the general consensus of opinion is that lower (acicular) bainite was found to be particularly susceptible to SCC. Chen and Thompson [Ref. 17] found that the presence of retained austenite, which was found in bainite I (upper bainite) was beneficial in reducing stress corrosion cracking. Bainite III (acicular or lower bainite) was found to be free of retained austenite, and stress corrosion cracking in HY-130 was found to occur in the weld metal-fusion line region, which was predominantly lower bainite and widely spaced martensitic laths. The fact that acicular bainite was found to be more susceptible to stress corrosion cracking is also pointed out in a later work of Chen, Bernstein and Thompson. [Ref. 17] Stoop and Metzbower

[Ref. 16] in their examination of stress corrosion cracking of HY-130 weldments found that acicular bainite was the predominant microstructure near the fracture edge in the SCC specimens. Boniszewski, et al. [Ref. 11] found that low carbon acicular bainite was particularly susceptible to hydrogen embrittlement and Mason [Ref. 20] found that cracking in HY-130 implant tests on the rolled plate used in this study (to determine levels of hydrogen embrittlement) occurred in the weld metal near the fusion line; the region of the acicular bainite microstructure. The presence of twinned martensite was found to be particularly susceptible to hydrogen embrittlement by Savage et al*, [Ref. 18] but only very small amounts of twinned martensite were observed in the present study, and these regions were always associated with upper bainite in the HAZ.

Failures of various HY-130 cast plates when tested by the explosion bulge test (EBT) described earlier in this work pointed to a lack of fracture toughness in HY-130 weldments. Brucker [Ref. 8] found that the HAZ toughness was considerably lower in both lower shelf energy and in a higher DBTT than that of the base metal. Holsberg Ref. 15] found a substantial reduction in fracture toughness in HY-130 weldments in the regions of upper bainite (Bainite I). These large packets of bainite with rod-shaped Widmanstatten carbides were observed in the region from 1.0mm. to 2.5mm. away from the fusion line in the

present study. Naylor and Krahe [Ref. 19] found that fracture toughness was decreased by the continuous precipitation of rod-shaped carbides in upper bainite, due also in part to the large irregular shape of the bainite in this morphology. Holsberg [Ref. 15] also pointed out that the low toughness upper bainite region has a lower hardness than martensite. This also was observed in the present work in the region of 1.0mm. to 2.5mm. away from the fusion line in figure (3-9).

Thus, it is felt that the low HAZ toughness in HY-130 weldments is due to the presence of upper bainite in the HAZ region near the fusion line. The conspicuous absence of upper bainite in the highest hardness region 2.5mm. to beyond 3.5mm. from the fusion line is believed to be caused by a lack of carbide solutioning during welding which results in an increase in the M_s temperature in this region of the weldment. If the HAZ temperature is higher than about 880°C complete solutioning of the carbides was observed and subsequent formation of upper bainite mixed with lath martensite was observed.

VI. CONCLUSIONS

1. No evidence of HAZ tempering by subsequent temper bead weld passes was observed in this study. However, the epsilon carbides that form initially upon tempering are possibly too small to be observed using the TEM available for this study.

2. The HAZ microstructures appeared essentially identical in regions where significant tempering would be expected and in regions where no tempering could have occurred. However, the HAZ hardness is lowered by the temper bead weld sequencing as is the steepness of the hardness gradient. A severe metallurgical notch is formed by the final weld pass when a straight bead welding sequence is used.

3. Hardness traverses in the HAZ of three different weldments, one rolled plate and two cast plates, indicate that plate #4, which failed the explosion bulge test, has a very severe metallurgical notch in the HAZ of the final weld pass (the location of the EBT failure).

4. The microstructure of the weld metal near the fusion line is heavily dislocated lower (acicular) bainite. This explains why most stress corrosion cracking failures occur in the weld metal dilution and thus the M_S is lower, allowing the formation of lower bainite.

5. The HAZ nearest the weld fusion line consists of a mixture of upper bainite with rod-shaped Widmanstatten carbides and fine lath martensite. This is believed to explain the low HAZ toughness in HY-130.

6. The HAZ nearest the base metal has a higher hardness than the HAZ nearer to the fusion line and consists mainly of fine lath martensite with coarse undissolved carbides. The number of carbides present increases as the base metal is approached. It is believed that the lower carbon content of the austenite during welding (due to the lack of dissolution of the large carbides) has raised the M_s temperature in this region preventing the formation of upper bainite.

7. The hardness of the fusion line has again been found to be lower than the HAZ and the weld metal adjacent to it, but no explanation for this observation has been found.

TABLE 1

CHEMICAL COMPOSITION OF ROLLED PLATE AND CAST PLATES

Alloy	Specification		Rolled Plate	Cast Plate 4	Cast Plate 6
	(Cast)	(Rolled)	(Rolled)	(Cast)	(Cast)
Nickel	5.25 - 5.5	4.75-5.25	4.82	5.64	5.25
Molybdenum	0.3 - 0.65	0.3 -0.65	0.51	0.44	0.52
Vanadium	0.05 - 0.1	0.05-0.1	0.08	0.05	0.11
Chromium	0.4 - 0.7	0.4 -0.7	0.57	0.53	0.57
Aluminum	0.015- 0.035	-	-	0.027	0.034
Titanium	0.02 (Max)	0.02 (Max)	0.01	0.02	0.02
Copper	0.25 (Max)	0.25 (Max)	0.08	0.19	0.07
Manganese	0.6 - 0.9	0.6 -0.9	0.75	0.75	0.77
Sulfur	0.008(Max)	0.01 (Max)	0.006	0.008	0.006
Phosporus	0.01 (Max)	0.01 (Max)	0.007	0.008	0.010
Silicon	0.2 - 0.5	0.2 -0.5	0.29	0.29	0.45
Carbon	0.12 (Max)	0.12 (Max)	0.10	0.09	0.12
Oxygen	100ppm max	-	-	26.00	43.00
Nitrogen	150ppm max	-	-	5.8	44.00
Hydrogen	10ppm max	-	-	5.1	5.5

TABLE 2

HEAT TREATMENT OF ROLLED PLATE AND CAST PLATE
#4 #6 HY-130 STEEL

Rolled Plate	Cast Plate #4	Cast Plate #6
Austenitize 830°C 3 hours, WQ	Normalize 1040°C 5 hours, Air Cool	Normalize 950°C 4 hours, Air Cool
Temper 620°C 3 hours, WQ	Austenitize 900°C 3 hours, WQ	Austenitize 900°C 3 hours, WQ
	Reaustenitize 840°C 5.5 hours, WQ	Reaustenitize 840°C 3 hours, WQ
	Temper 570°C 5.5 hours, WQ	Temper 600°C 3 hours, WQ
	Reaustenitize 900°C 5 hours, WQ	Retemper 620°C 5.5 hours, WQ
	Reaustenitize 840°C 5 hours, WQ	
	Retemper 590°C 5 hours, WQ	

TABLE 3

MECHANICAL PROPERTIES OF ROLLED PLATE AND CAST PLATE 4 and 6

Data	Target (Cast)	Target (Rolled)	Plate (Rolled)	Plate 4 (Cast)	Plate 6 (Cast)
Yield Strength (KSI)	130-145	130-145	134.1	133.7	127.3
Ultimate Strength (KSI)	(1)	(1)	144.6	144.5	143.5
% Elongation	15	15	19.5	15.5	16.5
% Reduction of Area	50	50	61.8	53	49.5
Impact Energy (-18°C) (Ft-lbs)	50	60	68	63.3	61
Impact Energy (Room Temp) (Ft-lbs)	(2)	(2)	73.3	72.5	67

(1) Recorded for Information Only
(2) Average CVN at room temperature shall not be more than 15ft-lbs above average at -18°C

TABLE 4

COMPOSITION AND PROPERTIES OF HY-130 WELD WIRE
(MIL - 1405-1)

Alloy	Weight %
Nickel	2.60
Molybdenum	0.93
Vanadium	0.011
Chromium	0.73
Aluminum	0.016
Titaniun	0.021
Copper	0.09
Manganese	1.63
Sulfur	0.006
Phosphorus	0.007
Silicon	0.44
Carbon	0.097
Zirconium	0.01

Minimum yield strength 135,000

TABLE 5

AVERAGE LATH WIDTHS IN MICRONS FOR MARTENSITE LATHS AND BAINITE LATHS IN MICROSTRUCTURES SHOWN IN FIGURES (11-19)

	Average lath widths, μm	
Location	Martensite	Bainite
Base Metal	.22 - .26	-
3.25mm. from Fusion Line	.18 - .22	-
2.5mm. from Fusion Line	.17 - .21	2.0 - 2.2 (a)
1.5mm. from Fusion Line	.15 - .19	2.0 - 2.2 (a)
1.0mm. from Fusion Line	.16 - .19	1.5 - 1.7 (a)
Fusion Line	-	.43- .52 (b)
Weld Metal	_	.48- .56

(a) Upper bainite (bainite I)
(b) Lower bainite (bainite III)

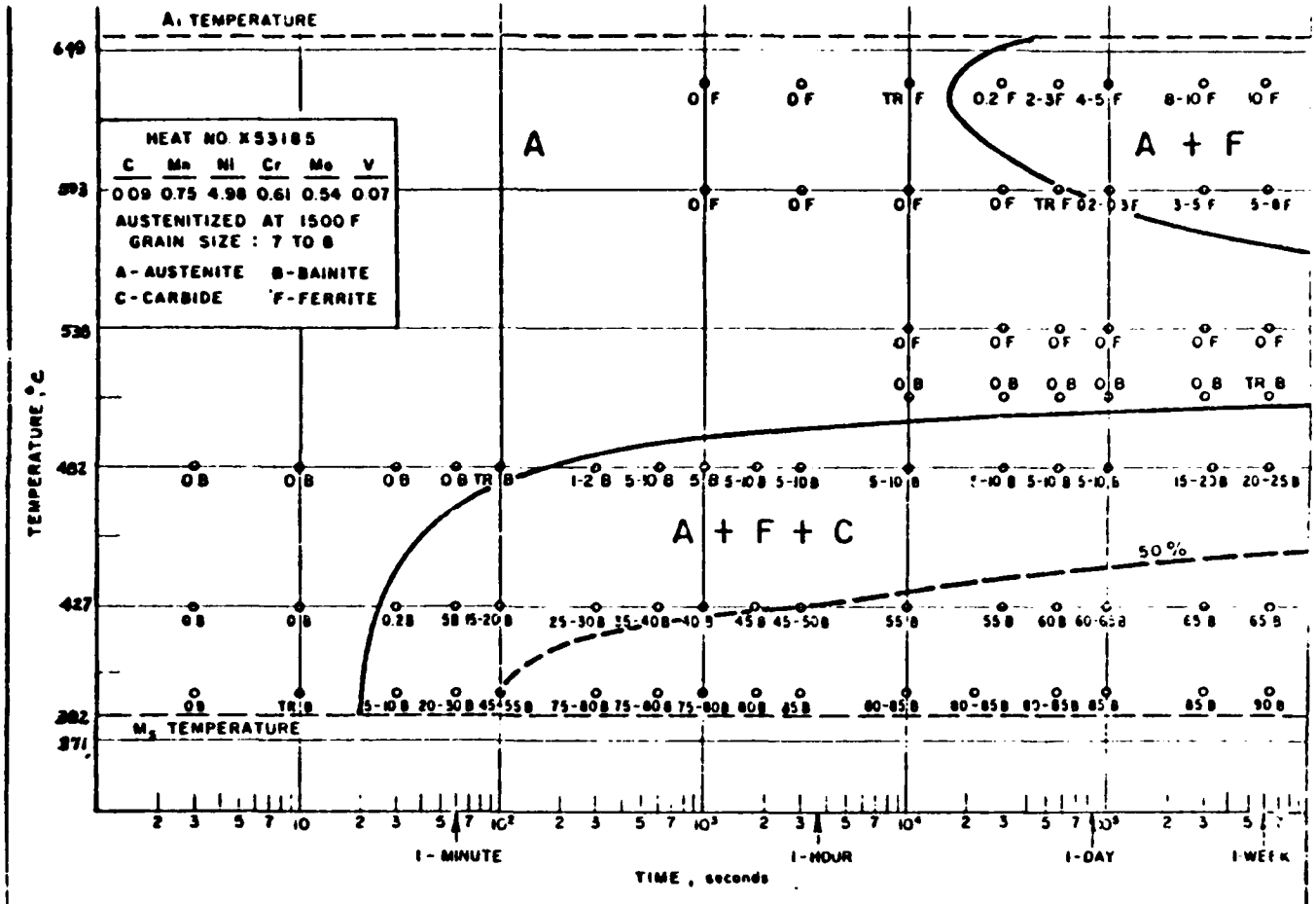

ISOTHERMAL - TRANSFORMATION DIAGRAM FOR HY - 130(T) STEEL

DRAWN BY	CHK'D BY	APPROVED BY	UNITED STATES STEEL CORPORATION	FIGURE NO
J D	S. J M	J H G	APPLIED RESEARCH	
DRAWING NO		PROJECT No	PITTSBURGH, PA.	
ARL 18-759		39 018 - 001 (64)		2.11
		DATE		
		1 - 21 - 66		

Figure 1

Figure 2

PHOTOGRAPH OF GMAW HY-130 WELDMENT IN 50mm THICK ROLLED PLATE SHOWING CONTRAST IN FUSION AND HAZ AREAS

Figure 3

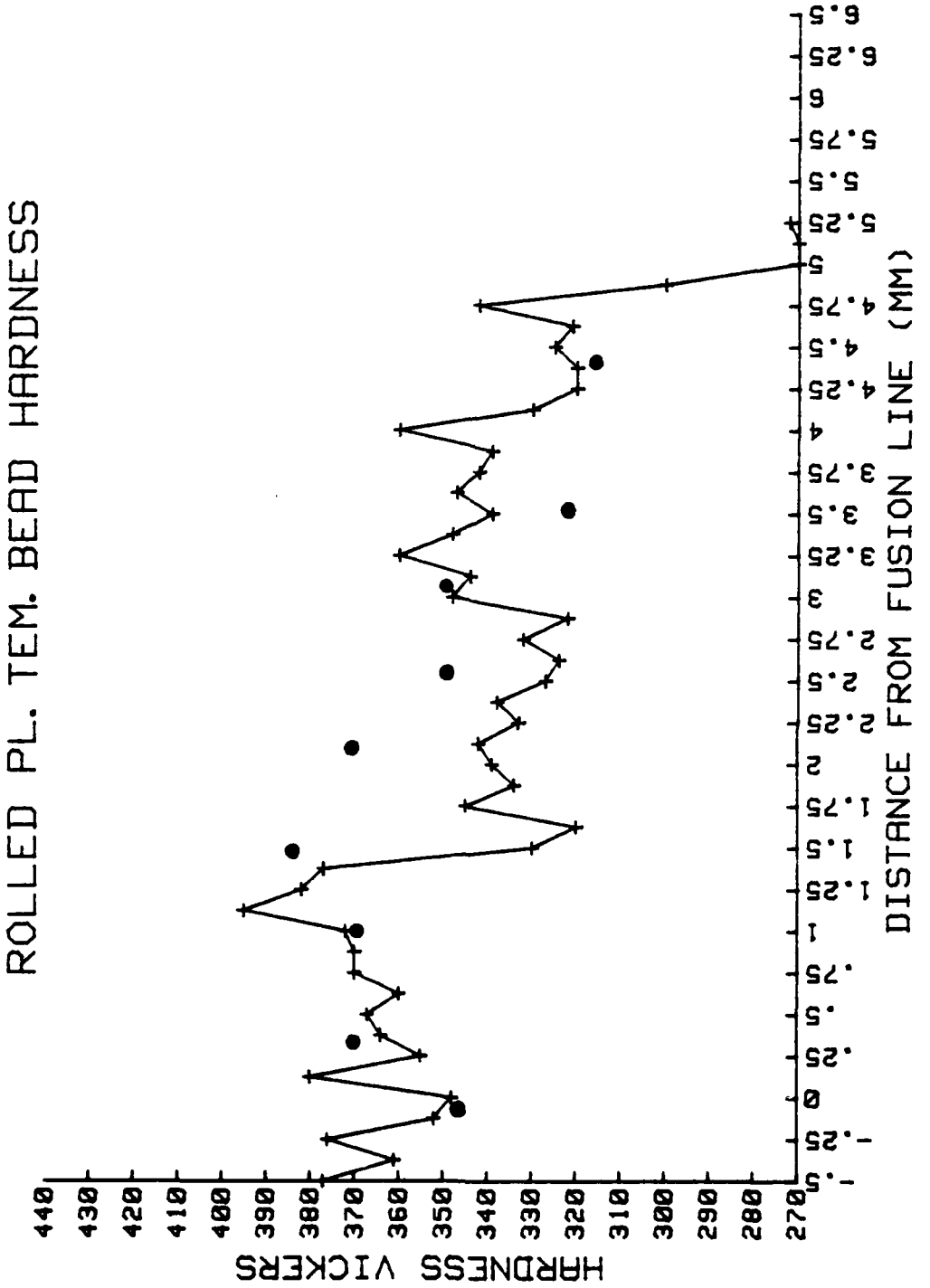

MICROHARDNESS TRAVERSE FOR ROLLED PLATE, REGION #2 (SOREK) WITH DOTS MARKING LOCATIONS OF THIN FOILS EXAMINED

Figure 4

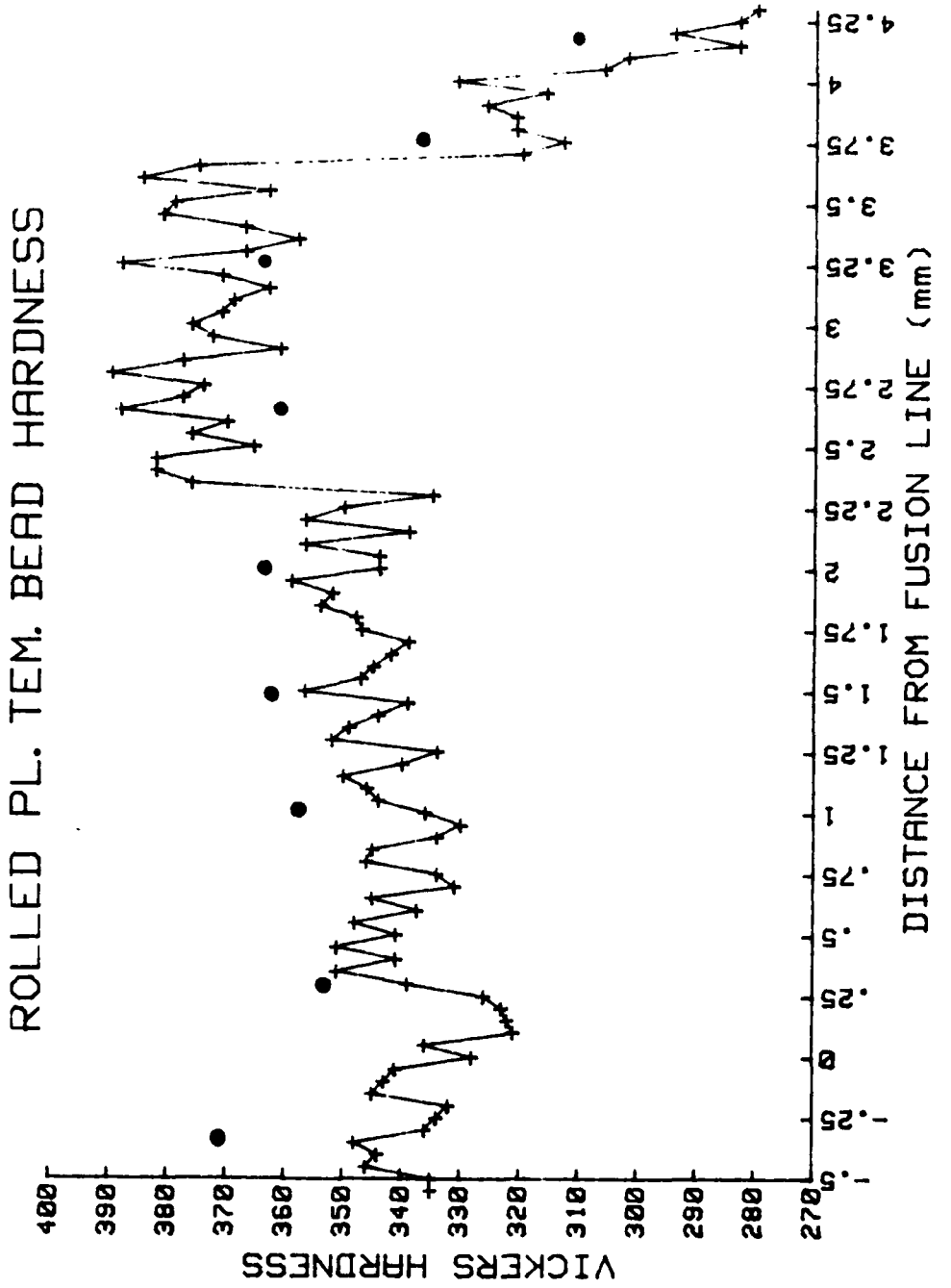

MICROHARDNESS TRAVERSE FOR ROLLED PLATE, REGION #4 (SOREK)
WITH DOTS MARKING LOCATIONS OF THIN FOILS EXAMINED

Figure 5

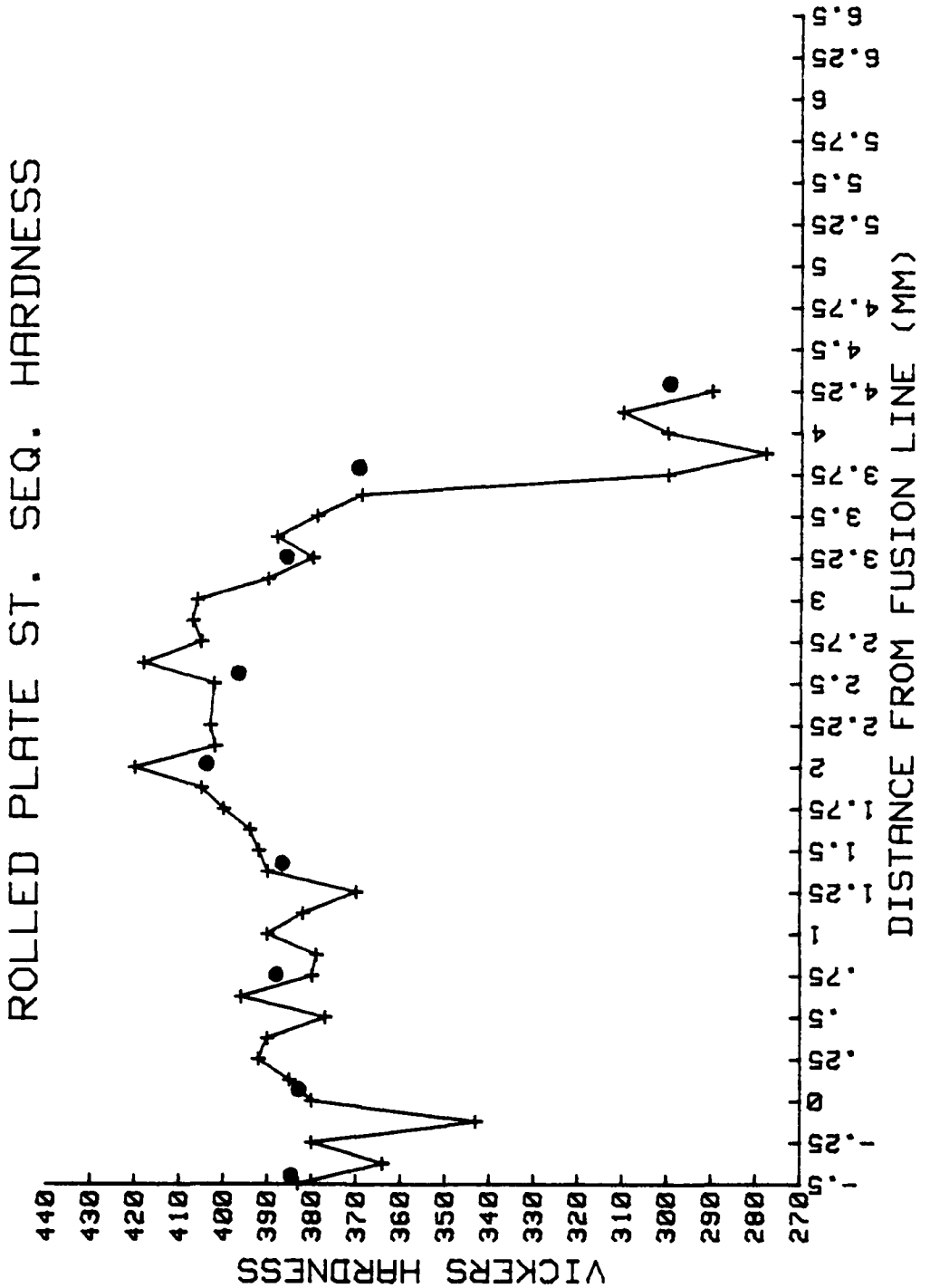

MICROHARDNESS TRAVERSE FOR ROLLED PLATE, REGION #3 (SOREK)
WITH DOTS MARKING LOCATIONS OF THIN FOILS EXAMINED

Figure 6

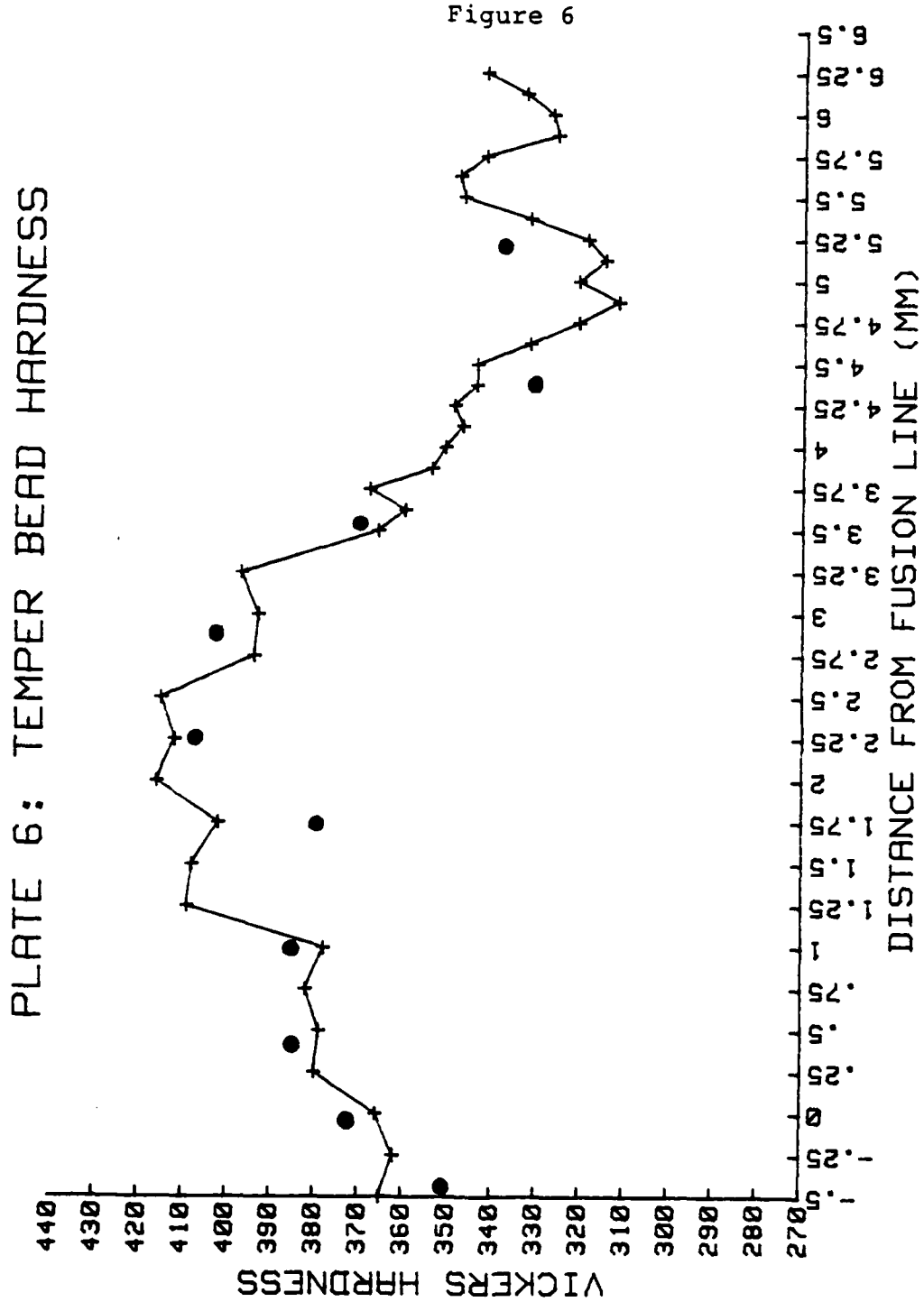

MICROHARDNESS TRAVERSE FOR CAST PLATE #6 WITH DOTS SHOWING POTENTIAL SITES FOR THIN FOIL EXAMINATION

Figure 7

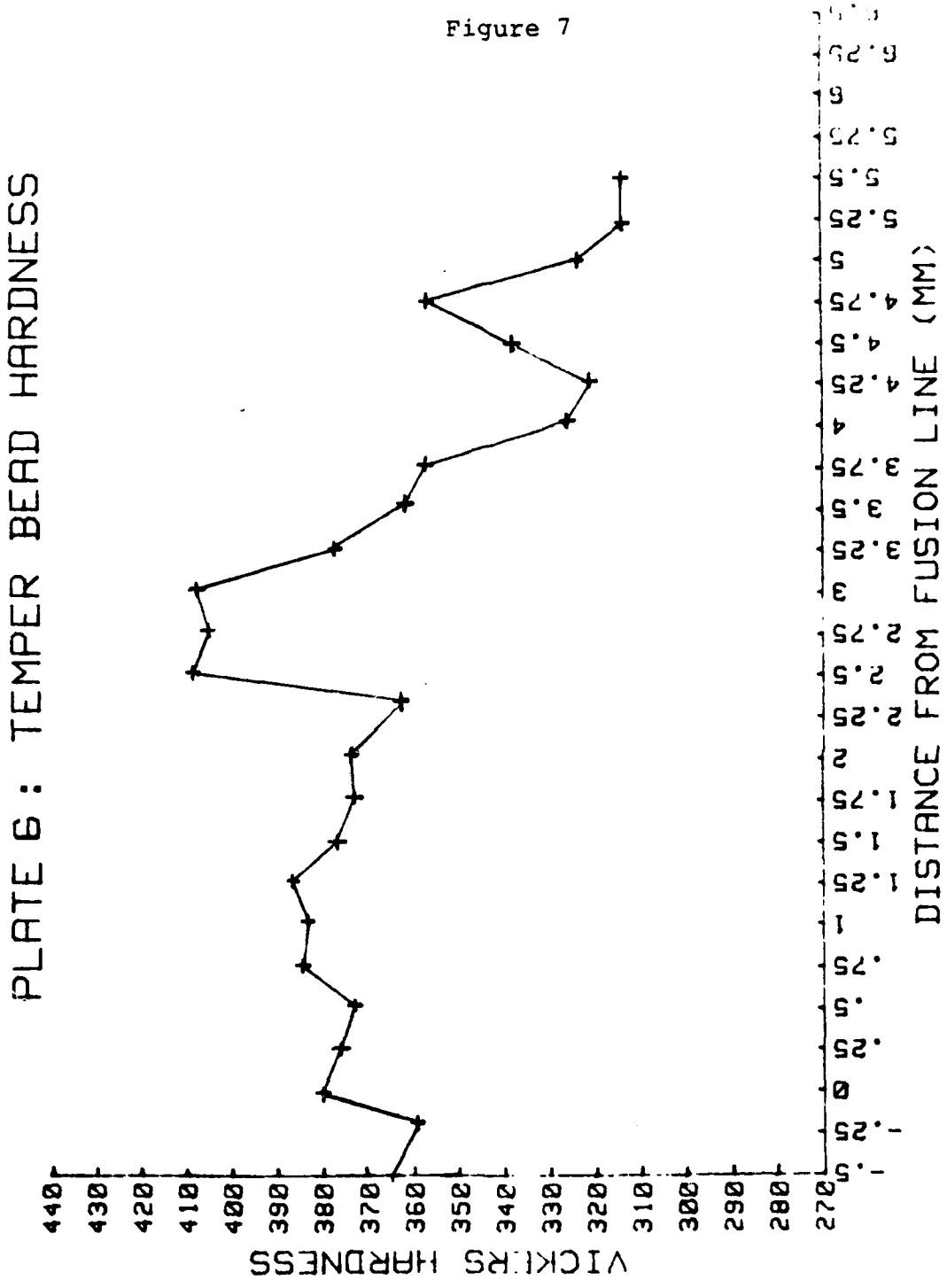

MICROHARDNESS TRAVERSE FOR CAST PLATE #6

Figure 8

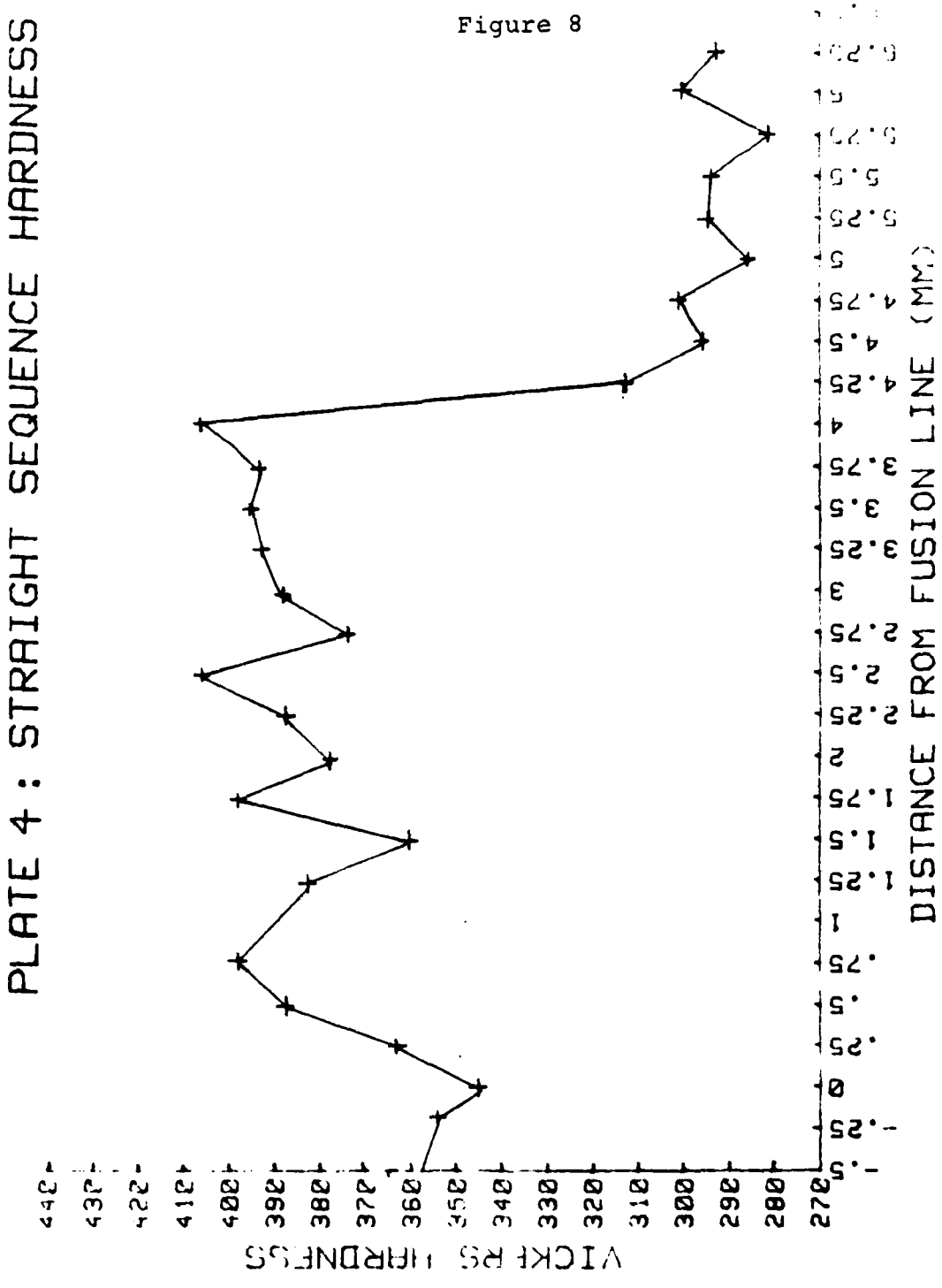

MICROHARDNESS TRAVERSE FOR CAST PLATE #4

Figure 9

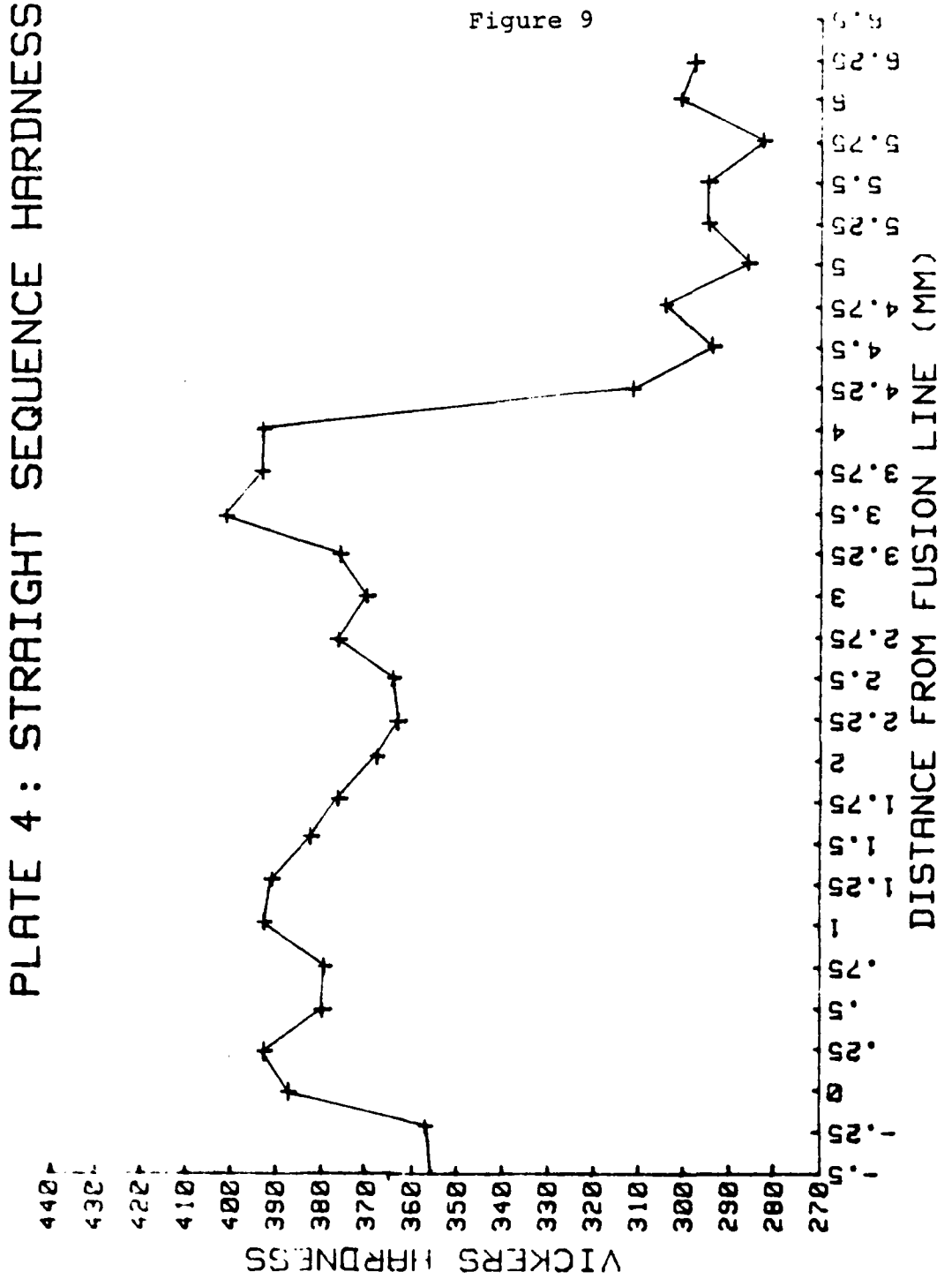

MICROHARDNESS TRAVERSE FOR CAST PLATE #4

Figure 10

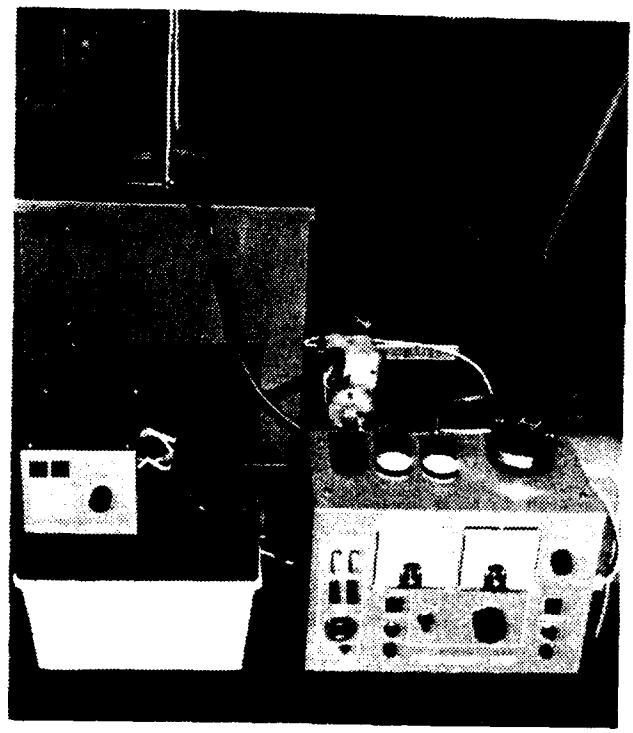

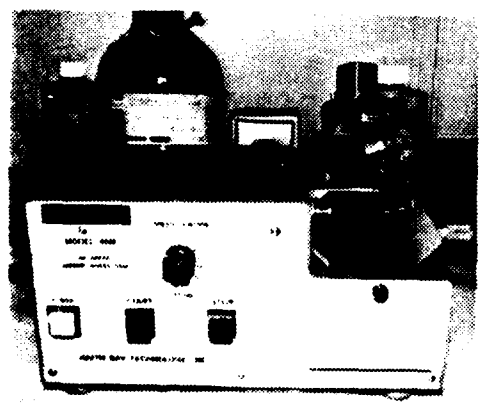

PHOTOGRAPH OF ELECTROPOLISHING UNIT AND LOW SPEED DIAMOND WAFERING SAW

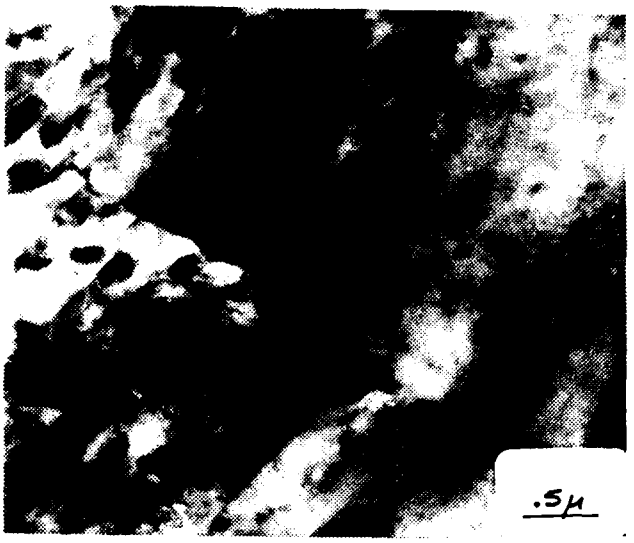

Figure 11

BASE METAL MICROSTRUCTURES, DESCRIBED IN TEXT, ALL PHOTOGRAPHS AT 22,000X WITH TEM

Region 2

Region 3

Region 4

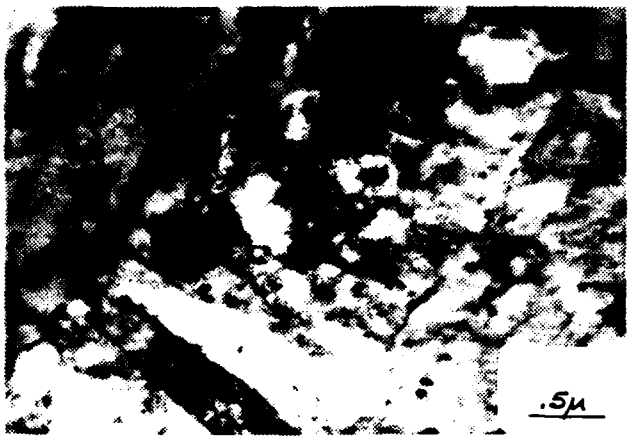

Figure 12

MICROSTRUCTURES AT 3.25mm. DISTANCE FROM FUSION LINE, ALL PHOTOGRAPHS AT 22,000X WITH TEM

Region 2

Region 3

Region 4

Figure 13

MICROSTRUCTURES AT 2.5mm. DISTANCE FROM FUSION LINE ALL PHOTOGRAPHS AT 22,000X WITH TEM

Region 2

Region 3

Region 4

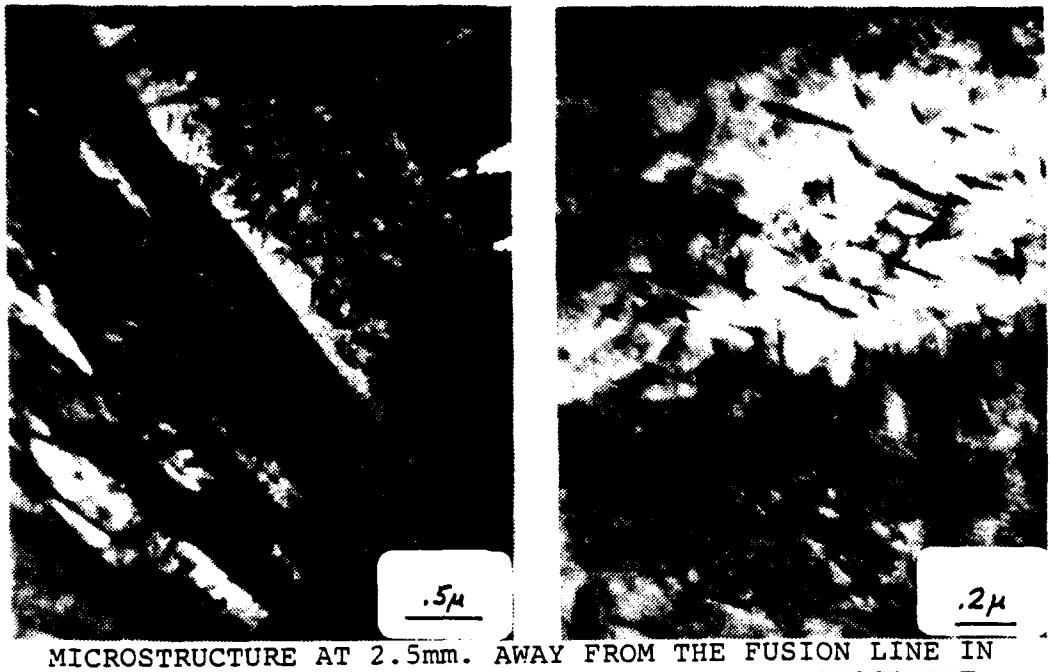

MICROSTRUCTURE AT 2.5mm. AWAY FROM THE FUSION LINE IN REGION 3 WITH THE PHOTO ON THE RIGHT AN ENLARGEMENT OF THE ROD-SHAPED WIDMANSTATTEN CARBIDES PRECIPITATED IN THE UPPER BAINITE ON THE LEFT

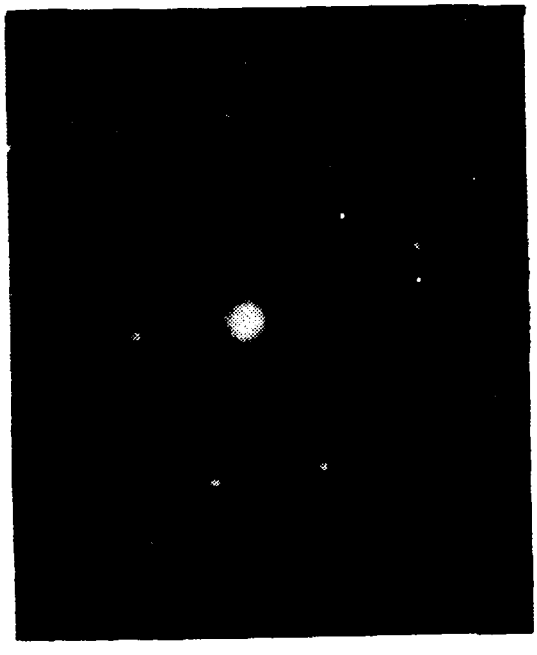

SELECTED AREA DIFFRACTION PATTERN SHOWING CARBIDES IN ENLARGED PHOTO AT RIGHT

Figure 14

Figure 15

MICROSTRUCTURES AT 1.5mm. DISTANCE FROM FUSION LINE, ALL PHOTOGRAPHS AT 22,000X WITH TEM

Region 2

Region 3

Region 4

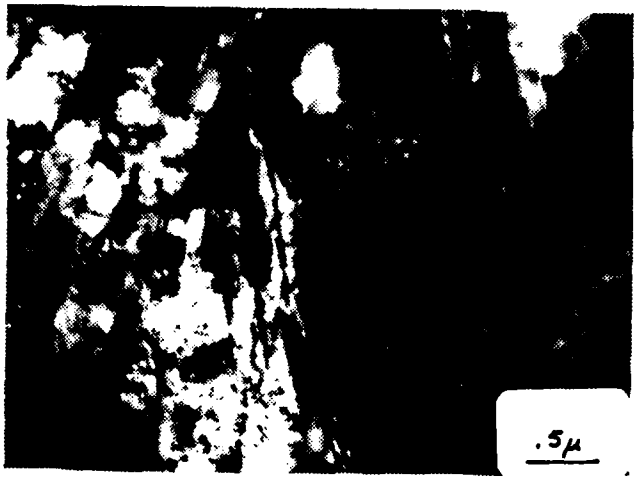

Figure 16

MICROSTRUCTURES AT 1.0mm. DISTANCE FROM FUSION LINE, ALL PHOTOGRAPHS AT 22,000X WITH TEM

Region 2

Region 3

Region 4

DARK FIELD BRIGHT FIELD

MICROSTRUCTURE SHOWING TWINNED MARTENSITE IN THE UPPER BAINITE OF REGION 4

SELECTED AREA DIFFRACTION OF ABOVE SHOWING TWINNED MARTENSITE

Figure 17

Figure 18

MICROSTRUCTURES AT FUSION LINE, ALL PHOTOGRAPHS AT 22,000X

Region 2

Region 3

Region 4

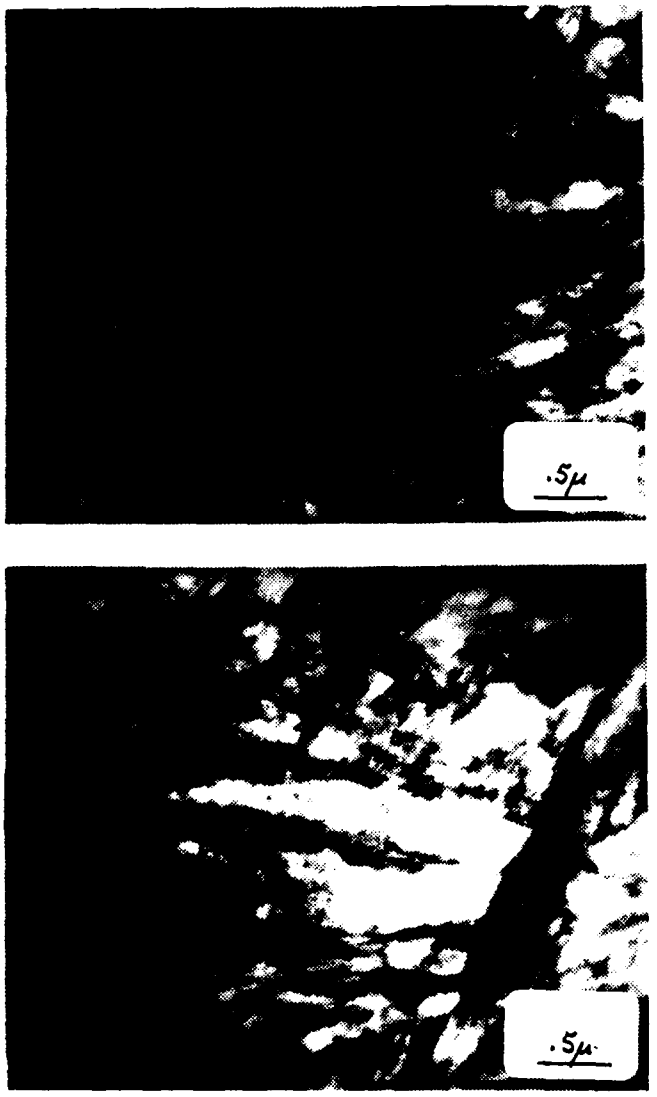

Figure 19

MICROSTRUCTURES IN THE WELD METAL, JUST INSIDE THE FUSION LINE, ALL PHOTOGRAPHS AT 22,000X WITH TEM

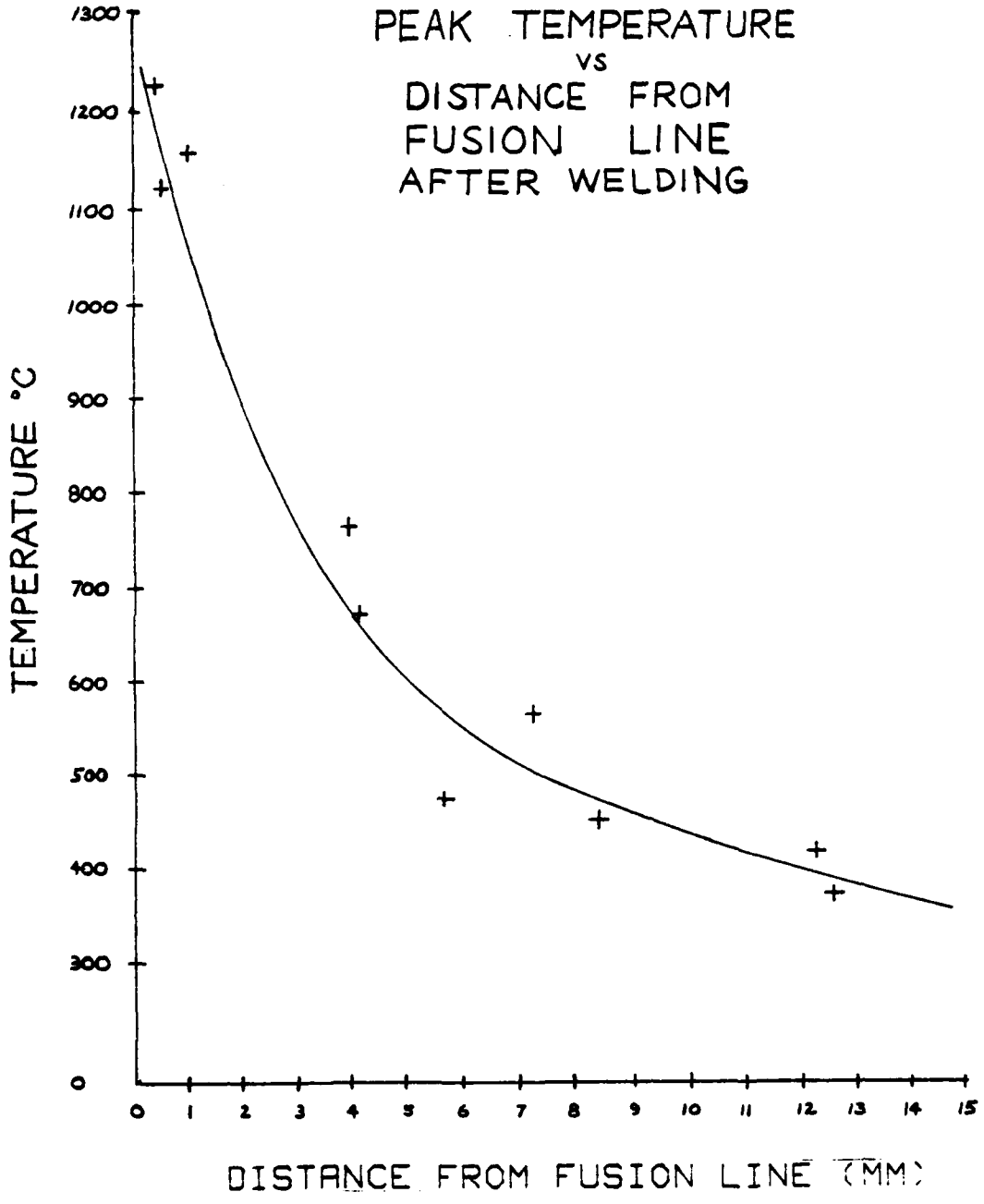
PEAK TEMPERATURE
VS
DISTANCE FROM
FUSION LINE
AFTER WELDING
TEMPERATURE °C
1300
1200
1100
1000
900
800
700
600
500
400
300
0
0 1 2 3 4 5 6 7 8 9 10 11 12 13 14 15
DISTANCE FROM FUSION LINE (MM)

Figure 20

Figure 21

PHOTOGRAPH OF GMAW HY-130 WELDMENT IN 50mm. THICK ROLLED PLATE WITH WELD GEOMETRY SUPERIMPOSED

APPENDIX A

PREPARATION OF THIN FOILS OF HY-130 (ROLLED) MATERIAL

In order to assist others in the preparation of thin foils of HY-130 rolled material, the following procedures which have proven successful are hereby recorded. Settings given are for use with the Struers Tenupol electropolishing apparatus, but techniques are easily transferred to other electropolishing equipment.

A. INITIAL CUTTING OF MATERIAL

Slices on the order of 0.1mm. thickness can be cut without bending in HY-130 because of the inherent strength of the material, but to be absolutely certain that bending does not occur, the material should be sliced to .015mm. thickness minimum. All edge burrs should be removed using 400 grit wet sanding paper.

B. ELECTRO THINNING

A solution of 5% Perchloric Acid-95% Acetic Acid was found to work best for electrothinning, electrocutting and electropolishing. Remember to pour the perchloric acid into the acetic acid upon initial mixing to avoid difficulties with chemical reactions between the two acids. Insert a slice of HY-130, maximum size 23mm. square X 1mm. thick into the 10mm. diameter specimen holder, connect the

electrical leads to the 2.5mm. jets and the holder, and turn on the power supply to provide about 80 volts (.9 amperes current) and a high (10) flow rate. Utilizing an external light source, watch the polishing action on the piece through the optical window, and remember to stop and measure the thickness of the now-thinned 10mm. diameter section periodically until it is of somewhat uniform .05mm. thickness. Polishing action favors the more rapid removal of material from the top of the specimen than from the bottom. It was found that specimens which completely fill the 10mm. diameter space polish more uniformly than those specimens with space on either side (less than 10mm. in width).

C. ELECTROCUTTING OF THIN FOIL DISKS

Electrolytically cutting 3mm. diameter disks of .05mm. nominal thickness was found to be superior to mechanically punching disks due to the distortion caused through mechanical deformation of the disk edges.

Struers manufactures a special acid-resistant adhesive tape from which 3mm. diameter disks of tape can be cut and attached to a clean, grease-free thinned slice in any pattern desired. These disks are attached to one side of the slice on the 10mm. diameter thinned area and the other side of the slice is completely covered with the tape. The tape must positively adhere to the surface or there will be etched and pitted areas in the non-adhering areas. The electrical lead which is normally attached to the 2.5mm.

diameter jet on the side completely covered with tape is not connected. Polishing (thinning) of the exposed metal around the tape disks is done at 110 volts (.5 amperes current), with a high (10) flow rate. Utilizing an external light source, monitor the preferential attack on the metal until only tape disks and backing tape are visible.

Remove the slice from the specimen holder and soak it in acetone until the tape floats free of the metal, then dry the specimen on a soft cloth or absorbent paper.

D. ELECTROPOLISHING THIN FOILS

Starting with a thin disk, 3mm. diameter and not greater than .05mm. thickness (remember that HY-130 is magnetic and will deflect the electron beam, so you want to have the smallest mass of material possible) insert the disk into the 3mm. specimen holder and snap the 1mm. jets and holder into place. If the 3mm. diameter disk is somewhat wedge shaped due to uneven electrothinning, place the thicker portion at the top of the 3mm. diameter specimen holder in order to gain a more uniform thickness upon final electropolishing. The thicker material at the top will polish faster than the bottom material.

Prior to commencing polishing, a photocell must be attached to the optical window. This device will terminate polishing whenever it detects light provided by the rheostat controlled light at the back of the polishing unit. To set the photocell, first set the rheostat to (7), this

will ensure that an adequately small hole is produced; second, with the electrical connections disconnected, turn on the pump and thin (current) switch and turn up the potentiometer until the buzzer sounds, then back off one and one-half to two graduations. Once the photocell has been set, connect the electrical leads, and begin polishing at a low (1.5) pump speed and 65 MA current. Polishing should take 60 to 120 seconds, then the buzzer will sound indicating a hole has been polished through the disk. Remove the specimen, and rinse in acetone, dry on a soft cloth and place in a glass container in a dessicator for later use. Storage of up to two months has been possible without deterioration of the foil through this method.

LIST OF REFERENCES

1. Dabkowski, D.S., Manganello, S.J., and Porter, L.F. "The Effect of Heat Treatment on the Strength and Toughness of Promising 130-to 150 KSI Yield-Strength Submarine Hull Steels," U.S. Steel Applied Research Lab Report 40.18-001, p. 2, March 1963.

2. Porter, L.F., Rathbone, A.M., et al. "The Development of an HY-130(T) Steel Weldment," U.S. Steel Applied Research Lab Report 39.018-001, pp. 3, 15,-17, June 1966.

3. Connor, L.P., Rathbone, A.M., Willebrand, C.F. "Effects of Composition on Heat Affected Zone Toughness of Ni-Cr-Mo Steel Weldments," U.S. Steel Applied Research Lab Report 39,018-008, pp. 16-17, Oct. 21, 1965.

4. Zanis, C.A., Palko, W.A., Byrne, J.P., "Processing of HY-130 Steel castings," American Foundrymen's Society Transactions, p. 194, Vol. 84, 1976.

5. Flax, R.W., Keith, R.E., Randall, M.D. "Welding the HY Steels," ASTM Special Technical Publication 494, Philadelphia, Pa., p. 13.

6. Department of the Navy Specification, "Standard Procedure for Preproduction Testing Materials by the Explosion Bulge Test," Revision 1, November 1965.

7. Rathbone, A.M. "Explosion Bulge Test of HY-80 and HY-130(T) Weldments Fabricated in the Vertical Position," U.S. Steel Corporation Technical Report on Project 39.018-006, May 1, 1967.

8. Brucker, R.B., "Fracture Properties of HY-130 Cast Plate Weldments," Master's Thesis, Naval Postgraduate School, pp. 24, 34, December 1980.

9. Sorek, M.J., "A Correlation Between the heat Affected Zone Microstructure and the Thermal History During Welding of HY-130 Steel," Master's Thesis, Naval Postgraduate School, September 1981.

10. Paulina, J.P. and Porter, L.F., "Microstructure in HY-130 Steel Plates," U.S. Steel Applied Research Lab Report 39.018-006, July 1, 1968.

11. Boniszewski, T., Watkinson, F., "Effect of Weld Microstructures on Hydrogen-Induced Cracking in Transformable Steels: Part I & II," Metals and Materials, pp. 90-151, March 1973.

12. Chen, C., Thompson, A.W. and Bernstein, I.M., "Microstructure and Stress Corrosion Cracking of Low Carbon Alloy Steel Welds. Part I: The Effect of Welding Variables on Microstructure of HY-130 Steels." Weldments: Physical Metallurgy and Failure Phenomena. Proceedings 5th Bolton Landing Conference, pp. 219-220, August 1978.

13. Donachie, S.J., and Ansell, G.S., "The Effect of Quench Rate on the Properties and Morphology of Ferrous Martensite," Metallurgical Transactions, Volume 6A, pp. 1863-1875, October 1975.

14. Speich, G.R., "Tempering of Low Carbon Martensite," AIME, Volume 245, pp. 2553-2563.

15. Holsberg, P.W., "High Strength Steel Weldment Subcritical Cracking Problem--Relationship of Transformations, Microstructure and Properties in the HY-130 System," Ship Materials Engineering Department Research and Development Report, DTNSRDC, July 1979.

16. Stoop, J. and Metzbower, E.A., "A Metallurgical Characterization of HY-130 Steel Welds," Welding Research Supplement, Vol. 57, No. 11, Nov. 1976.

17. Chen, C., Thompson, A.W., Bernstein, I.M., "The Correlation of Microstructure and Stress Corrosion Fracture of HY-130 Steel Weldments," Metallurgical Transactions, Vol. 11A, pp. 1723-1730, October 1980.

18. Savage, W.F., Nippes, E.F., and Szekeres, E.S., "A Study of Weld Interface Phenomena in a Low Alloy Steel," Welding Research Supplement, pp. 260-268, September 1976.

19. Naylor and Krahe, "The Effect of Bainite Packet Size on Alloy Toughness," Metallurgical Transactions, Vol. 5, pp. 1699-1700, 1974.

20. Mason, B.J., "Use of Implant Testing to Evaluate the Susceptibility of HY-130 Steel Weldments to Hydrogen Embrittlement," Master's Thesis, Naval Postgraduate School, December 1981.

INITIAL DISTRIBUTION LIST

		No. Copies
1.	Defense Technical Information Center Cameron Station Alexandria, Virginia 22314	2
2.	Library, Code 0142 Naval Postgraduate School Monterey, California 93940	2
3.	Department Chairman, Code 69 Department of Mechanical Engineering Naval Postgraduate School Monterey, California 93940	1
4.	Assistant Professor K.D. Challenger, Code 69Ch Department of Mechanical Engineering Naval Postgraduate School Monterey, California 93940	5
5.	Dr. Charles Zanis, Code 2820 David Taylor Research and Development Center Annapolis, Marland 21402	1
6.	Mr. Ivo Fioritti, Code 323 Naval Sea Systems Command National Center, Building 3 2531 Jefferson Davis Highway Arlington, Virginia 20362	1
7.	Lt. Wallace M. Elger USN 1256 Lenape Avenue Ford City, Pennsylvania 16226	2
8.	Mr. Jess Elger Process Metallurgist U.S. Steel-Irvin Works Box 878 Dravosburg, Pennsylvania 15034	1


DATE
ILME
8